Engineering Hydrophobic Covalent Organic Frameworks for Electroreduction of Nitrate to Ammonia

Fuzhen Li,[a] Huan Lin,[c] Chunying Chen,[c] Li-lin Tan,[b] Dawei Wang,[c] Cunyuan Zhao,[c] Li Zhang*[c], Cheng-Yong Su[c]

[a]School of Chemical Engineering and Technology, Sun Yat-sen University, Zhuhai 519082, China

[b]Shantou Engineering Technology Research Center for Green and Precise Manufacturing of High-value Chemicals, Chemistry and Chemical Engineering Guangdong Laboratory, Shantou 515031, China

[c]Lehn Institute of Functional Materials, School of Chemistry, Sun Yat-Sen University, Guangzhou 510006, China. E-mail: zhli99@mail.sysu.edu.cn

Contents

Captions for Figures and Tables

Figure 20. ABC stacking model of PCOF-2(Cu_3) viewed from *c* axis. The orange, dark blue, red and white spheres refer to copper, nitrogen, oxygen and hydrogen, respectively.

Figure S21. SEM images of Pd-PCOF-1(Cu_3).

Figure S22. SEM images of Pd-PCOF-2(Cu_3).

Figure S23. SEM images of PCOF-2(Cu_3).

Figure S24. FT-IR spectra of Pd-PCOF-1(Cu_3), $Cu_3(PyCA)_3$ and Pd-DAPP.

Figure S25. FT-IR spectra of Pd-PCOF-2(Cu_3), $Cu_3(PyCA)_3$ and Pd-EDAPP.

Figure S26. FT-IR spectra of PCOF-2(Cu_3), $Cu_3(PyCA)_3$ and EDAPP.

Figure S27. Pore size distribution profiles of Pd-PCOF-1(Cu_3) (a), Pd-PCOF-2(Cu_3) (b) and PCOF-2(Cu_3) (c) calculated by Nonlocal Density Functional Theory (NLDFT) modeling based on N_2 adsorption data.

Figure S28. Survey scan XPS profiles of $Cu_3(PyCA)_3$ (a), Pd-EDAPP (b), Pd-PCOF-1(Cu_3) (c), Pd-PCOF-2(Cu_3) (d) and PCOF-2(Cu_3) (e).

Figure S29. High-resolution Cu *2p* XPS profiles of $Cu_3(PyCA)_3$ (a), Pd-PCOF-1(Cu_3) (b), Pd-PCOF-2(Cu_3) (c) and PCOF-2(Cu_3) (d).

Figure S30. High-resolution Pd *3d* XPS profiles of Pd-EDAPP(a), Pd-PCOF-1(Cu_3) (b) and Pd-PCOF-2(Cu_3) (c).

Figure S31. TGA curves of Pd-PCOF-1(Cu_3) (a), Pd-PCOF-2(Cu_3) (b) and PCOF-2(Cu_3) (c) under N_2 atmosphere.

Figure S32. PXRD patterns of Pd-PCOF-2(Cu_3) after treatment with various solvents for 24 h.

Figure S33. PXRD patterns of PCOF-2(Cu_3) after treatment with various solvents for 24 h.

Figure S34. PXRD patterns of Pd-PCOF-1(Cu_3) after treatment with various solvents for 24 h.

Figure S35. Three-electrode H-type electrolytic cell for NO_3RR.

Figure S36. UV-vis absorption spectra of a series of standard KNO_2 solutions (a) and corresponding calibration curve used for the calculation of NO_2^- concentration (b). The inset is the photograph of the KNO_2 solution after chromogenic reaction.

Figure S37. UV-vis absorption spectra of a series of standard NH_4Cl solutions (a) and corresponding calibration curve used for the calculation of NH_3 concentration (b). The inset is the

photograph of the NH_4Cl solution after chromogenic reaction.

Figure S38. ^1H NMR spectra of $^{14}NH_4^+$ ions at different concentrations with 2 mM maleic acid as internal standard (a) and corresponding calibration curve used for the calculation of $^{14}NH_4^+$ concentration (b). The inset is the chemical construction of maleic acid.

Figure S39. ^1H NMR spectra of $^{15}NH_4^+$ ions at different concentrations with 2 mM maleic acid as internal standard (a) and corresponding calibration curve used for the calculation of $^{15}NH_4^+$ concentration (b).

Figure S40. Chronoamperometry curve of Pd-PCOF-1(Cu_3) for NO_3RR at different applied potentials (a). UV-vis absorption spectra of NO_2^- after chromogenic reaction (b).

Figure S41. Chronoamperometry curve of Pd-PCOF-2(Cu_3) for NO_3RR at different applied potentials (a). UV-vis absorption spectra of NO_2^- after chromogenic reaction (b).

Figure S42. Chronoamperometry curve of PCOF-2(Cu_3) for NO_3RR at different applied potentials (a). UV-vis absorption spectra of NO_2^- after chromogenic reaction (b).

Figure S43. The current density curve of Pd-PCOF-2(Cu_3) for continuous cyclic electrolysis at -0.9 V vs. RHE.

Figure S44. PXRD patterns of Pd-PCOF-2(Cu_3) before and after electrocatalysis over 10 consecutive cycles.

Figure S45. LSV curve at a scan rate of 10 mV s^{-1} (a) and chronoamperometry curve at -0.9 V vs. RHE (b) of Pd-PCOF-2(Cu_3) in 1 M KOH with 0.082 M $K^{15}NO_3$. The NH_3 FE of Pd-PCOF-2(Cu_3) after electrolysis using $^{14}NO_3^-$ or $^{15}NO_3^-$ as nitrogen resources at -0.9 V vs. RHE (c).

Figure S46. Nyquist plots of Pd-PCOF-1(Cu_3), Pd-PCOF-2(Cu_3) and PCOF-2(Cu_3) in 1 M KOH and containing 0.1 M KNO_3.

Figure S47. CV curves of Pd-PCOF-1(Cu_3) (a), Pd-PCOF-2(Cu_3) (b) and PCOF-2(Cu_3) (c) at different scan rates. CV current density versus scan rate (the liner slope is equivalent to the C_{dl}) (d). The ECSA comparison of Pd-PCOF-1(Cu_3), Pd-PCOF-2(Cu_3) and PCOF-2(Cu_3) (e).

Figure S48. The integrated area of $^*H_{ads}$ from the peak of the CV curves over Pd-PCOF-1(Cu_3) (a), Pd-PCOF-2(Cu_3) (b) and PCOF-2(Cu_3) in 1 M KOH.

Figure S49. LSV curve at a scan rate of 10 mV s^{-1} (a) and chronoamperometry curve at different

1. General information

All reagents and materials were commercially purchased and directly used without further purification. 1H-pyrazole-4-carbaldehyde, cupric nitrate trihydrate ($Cu(NO_3)_2 \cdot 3H_2O$), 4-nitrobenzaldehyde, propionic acid, stannous chloride dihydrate ($SnCl_2 \cdot 2H_2O$), sodium citrate and salicylic acid were purchased from Shanghai Aladdin Biochemical Technology Co., Ltd. *N*,*N*-dimethylformamide, ethanol, triethylamine, methanol, tetrahydrofuran, ammonia water and ammonium chloride were obtained from Shanghai Titan Scientific Co., Ltd. Pyrrole, dimethyl sulfoxide-d_6, chloroform-d, phosphoric acid (85%) and sodium nitroferricyanide dihydrate were purchased from Annaiji Chemical Co., Ltd. Trifluoroacetic acid, *N*-(1-naphthyl) ethyldiamine dihydrochloride and sodium hypochlorite (0.1 M) were purchased from Shanghai Macklin Biochemical Co., Ltd. Benzaldehyde, 4-ethoxybenzaldehyde and ammonium chloride-^{15}N were obtained from Bide Pharmatech Co., Ltd. Dichloromethane and petroleum ether (60-90 ℃) were purchased from Shanghai wohua-chemical Co., Ltd. o-Dichlorobenzene and n-butanol were obtained from J&K Scientific Co., Ltd. Potassium nitrate and concentrated hydrochloric acid were purchased from Guangzhou Chemical Reagent Factory. Acetone was obtained from Xilong scientific Co., Ltd. Palladium chloride ($PdCl_2$) was purchased from Kunming Boren Precious Metals Co.Ltd. Potassium hydroxide was obtained from Meryer (Shanghai) Chemical Technology Co., Ltd. Potassium nitrate-N^{15} was purchased from Wuhan Isotope Technology Co., Ltd. *p*-aminobenzene sulfonamide was obtained from Shanghai ACMEC Biochemical Co., Ltd.

Powder X-ray diffraction (PXRD) patterns of the samples are carried out on a Rigaku Smart Lab diffractometer (Bragg-Brentano geometry, Cu-Kα radiation, λ = 1.54056 Å), the detecting angles started from 2θ = 2.0 ° to 2θ = 40.0 °, with 0.02 °increment and a scan rate of 2.0 °/min or 10.0 °/min. Scanning electron microscope (SEM) and energy-dispersive X-ray spectroscopy images were recorded on a Hitachi S4800 with an accelerating voltage of 10.0 kV. Transmission electron microscope (TEM) images were obtained with FEI Tecnai G2 spirit (120 kV). X-ray photoelectron spectroscopy (XPS) measurement was performed on a ULVAC PHI Quantera microprobe. Fourier-transform infrared (FT-IR) spectra were recorded by PerkinElmer Frontier spectrometer with Attenuated Total Reflectance (ATR) mode. The spectra are collected at 1 cm^{-1}

resolution over 16 scans. Solid state ^{13}C cross-polarization magic angle spinning nuclear magnetic resonance spectrum (^{13}C CP-MAS NMR) was measured on Bruker Avance Neo 600. Thermogravimetric analysis (TGA) was conducted on Netzsch TGA209F1 Thermogravimetric Analyzer and the samples were heated at a rate of 10.0 ℃·min^{-1} from 40.0 ℃ to 800.0 ℃ under the protection of nitrogen. Nuclear magnetic resonance (^{1}H NMR) spectra were performed by Bruker Advance III 400 (400 MHz) NMR spectrometer at room temperature. Ultraviolet and visible (UV-vis) absorption spectra were carried out on SHIMADZU UV-3600. Nitrogen sorption isotherms were measured with BSD-660M A6B3M physical adsorption analyze (Beishide Instrument Technology) at 77 K and samples were typically heated at 120 ℃ under vacuum for 12 h before test. The surface areas of samples were evaluated according to Brunauer-Emmett-Teller (BET) theory, the pore size distribution (PSD) was calculated by Nonlocal Density Functional Theory (NLDFT) modeling based on N_2 adsorption data. The static water contact angles were measured on OCA50 of Dataphysics Instrument GmbH.

2. Comparison of electrocatalytic NO_3RR performances of different materials

Table S1. Comparison of NH_3 yield rate and FE of Pd-PCOF-2(Cu_3) with reported COF and MOF-based electrocatalysts.

Catalyst	Electrolyte	Potential (V vs. RHE)	FE (%)	NH_3 yeild (mg h^{-1} cm^{-2})	Ref.
Pd-PCOF-2(Cu_3)	**1 M KOH + 0.1 M KNO_3**	**-1.0** **-1.1**	**94.70** **92.83**	**13.72** **15.09**	**This work**
NiPr-TPA-COF	0.5 M K_2SO_4 + 0.1 M KNO_3	-0.766	80	2.5	[1]
COF-366-Fe	0.5 M K_2SO_4 + 0.1 M KNO_3	-1.05	85.4	2.88	[2]
TTA-TPH-CuCo	0.5 M K_2SO_4 + 0.1 M KNO_3	-0.75	92.31	13.49	[3]
TpBpy-Cu-F	0.5 M Na_2SO_4 + 0.1 M $NaNO_3$	-0.746	82.6	2.72	[4]
Mo-HATN-COFs	0.5 M Na_2SO_4 + 0.1 M $NaNO_3$	-0.4	91.3	6.6	[5]
NiPc-CZDM-COF	0.5 M K_2SO_4 + 0.1 M KNO_3	-1.2	96.6	19.5	[6]
CuPOR-COF	1 M KOH + 1 M KNO_3	-0.67	86	6.0	[7]
ImPy-COF-Mn	NO_3^- (2mg mL^{-1}) + 1 M KOH + 0.5 M KF	-0.7	95.64	6.43	[8]
NiTP-CoTAPP MCOF	0.5 M KNO_3	-0.8	85.6	1.09	[9]
Zn_5-NiS_4TP MOF	0.05 M K_2SO_4 + 0.5 M KNO_3	-1.2	92.87	4.15	[10]
Cu-O_2N_2-MOF	0.1 M KOH + 0.1 M KNO_3	-0.7	96.28	2.62	[11]
Ni-BDC@Co-HHTP	1 M KOH + 0.1 M $NaNO_3$	-0.7	98.4	11.46	[12]
CoFe-cMOFs	1 M Na_2SO_4 + 0.5 M KNO_3	-0.7	94.3	14.1	[13]
NJUZ-2	0.1 M Na_2SO_4 + 0.1 M KNO_3	-0.8	98.4	1.76	[14]
Co-TATB	0.1 M Na_2SO_4 + 0.1 M KNO_3	-1.0	97.2	2.58	[15]
HUST-38	0.5 M K_2SO_4 + 0.1 M KNO_3	-0.6	95.7	2.01	[16]
Cu_1Co_1HHTP	0.5 M Na_2SO_4 + 0.1 M $NaNO_3$	-0.6	96.4	5.1	[17]
DiMe-Cu_3-MOF	0.5 M K_2SO_4 + 0.05 M KNO_3	-0.94	95	7.48	[18]

3. Synthesis and characterizations of PCOFs

3.1 Synthesis of 2,2'-((4-nitrophenyl)methylene)bis(1H-pyrrole) (NPBPR)

NPBPR was synthesized according to the literature[19]. Briefly, 4-Nitrobenzaldehyde (6.04 g, 0.04 mol) and pyrrole (83 mL, 1.2 mol) were added to a 250 mL round-bottom flask, followed by the slowly addition of 1 mL trifluoroacetic acid (TFA). The mixture was stirred at room temperature under darkness. After 1 h, the reaction was quenched with triethylamine (TEA), and the excess pyrrole was removed under reduced pressure. The crude product was purified by column chromatography (silica, dichloromethane (CH_2Cl_2)) to afford NPBPR as bright yellow solid (5.87 g, 55% yield). ^{1}H NMR (400 MHz, Chloroform-*d*) δ 8.19 (d, J = 8.8 Hz, 2H), 8.01 (s, 2H), 7.40 (d, J = 8.7 Hz, 2H), 6.77 (td, J = 2.7, 1.5 Hz, 2H), 6.20 (q, J = 2.9 Hz, 2H), 5.94 - 5.85 (m, 2H), 5.61 (s, 1H).

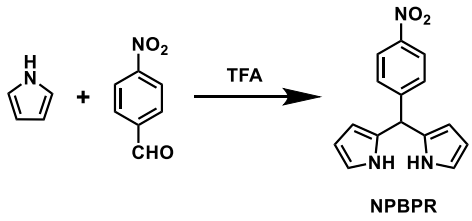

Figure S1. Schematic illustration of the synthesis of NPBPR.

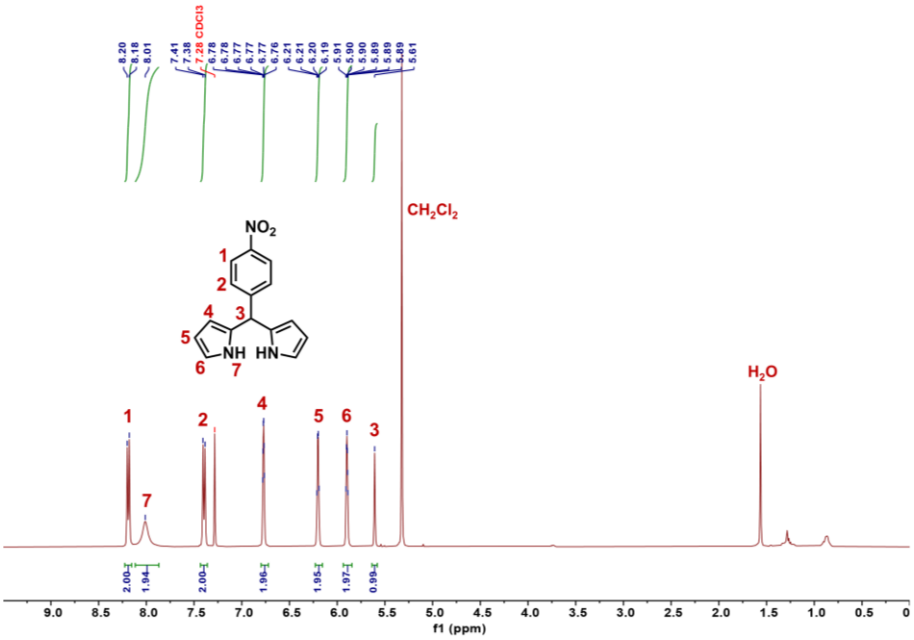

Figure S2. ^{1}H NMR spectrum of NPBPR in $CDCl_3$.

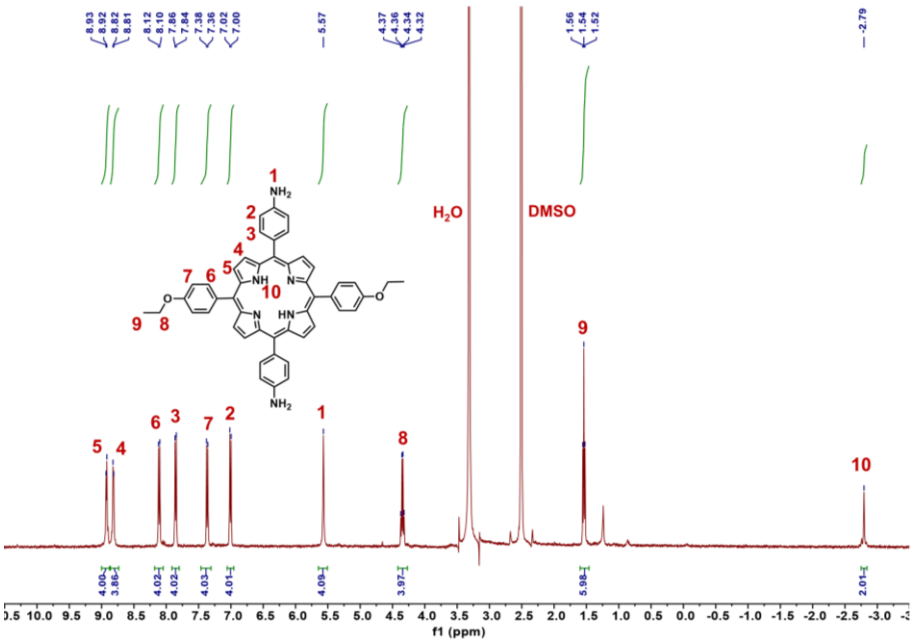

Figure S3. ^{1}H NMR spectrum of EDAPP in DMSO-d_6.

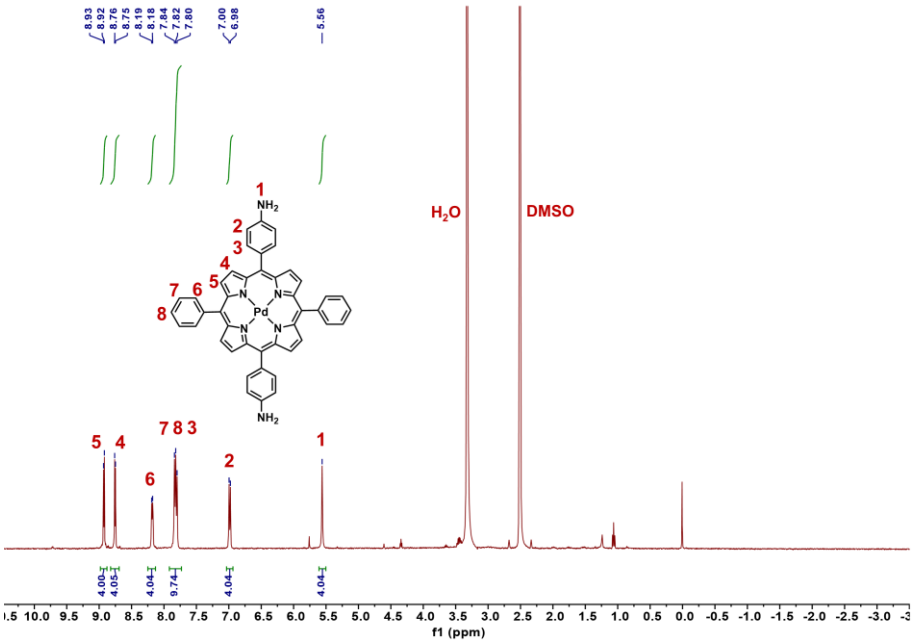

Figure S4. ^{1}H NMR spectra of Pd-DAPP in DMSO-d_6.

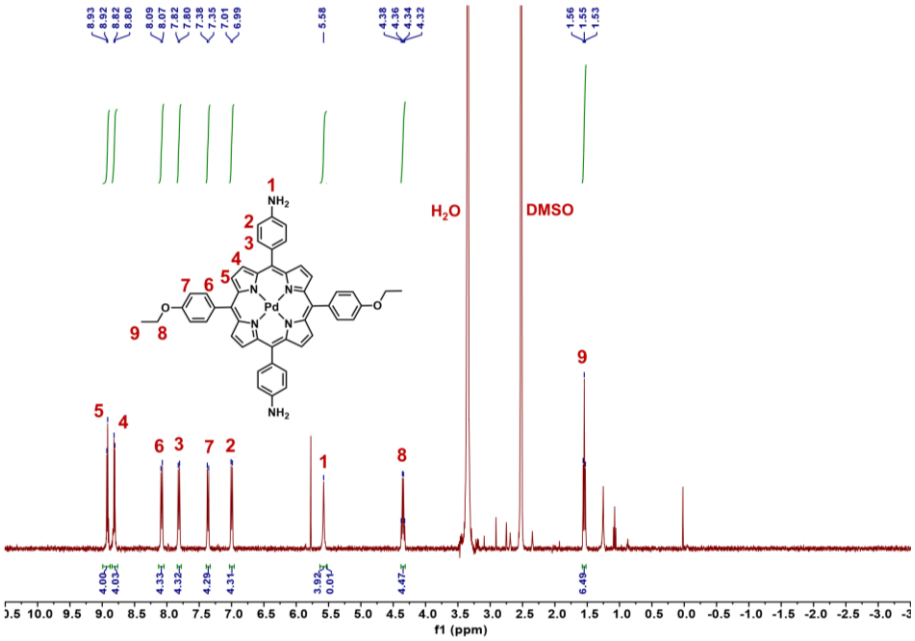

Figure S5. ^{1}H NMR spectrum of Pd-EDAPP in DMSO-d_6.

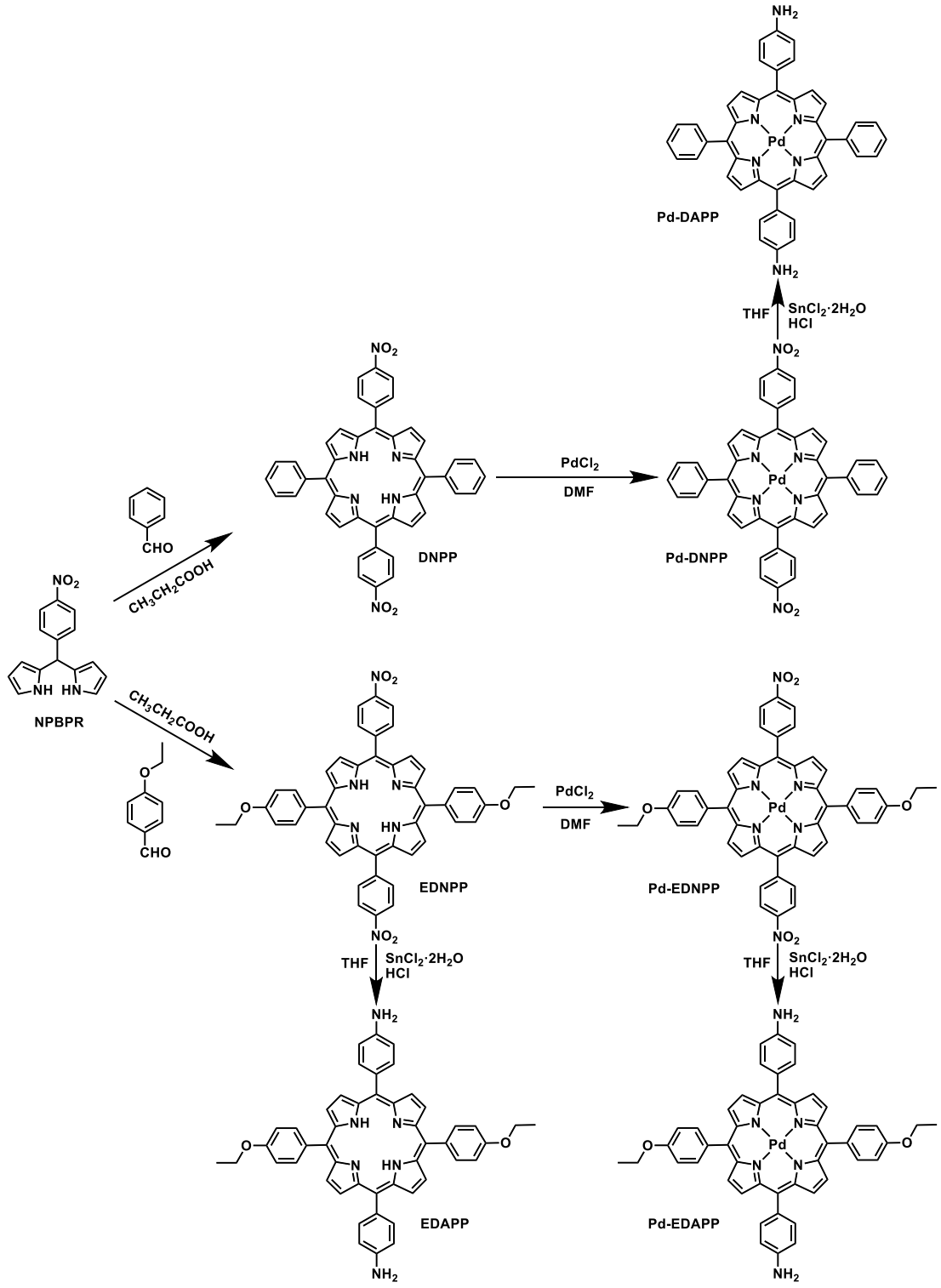

Figure S6. Schematic illustration of the synthesis of Pd-DAPP, Pd-EDAPP and EDAPP.

3.2 Synthesis of $Cu_3(PyCA)_3$

$Cu_3(PyCA)_3$ (PyCA = 1H-pyrazole-4-carbaldehyde) was prepared according to previously reported procedures.[20] $Cu(NO_3)_2$ $3H_2O$ (0.2 g, 0.83 mmol) and 1H-pyrazole-4-carbaldehyde (0.096 g, 1.0 mmol) were added to a 20 mL sample vial and 6.7 mL *N*, *N*-dimethylformamide (DMF), 6.7 mL ethanol (EtOH), and 5.0 mL H_2O were subsequently added to the vial. After being sonicated for 10 min, the mixture was left in an oven at 100 ℃ for 12 h and then cooled down to room temperature. The light-yellow single crystals were collected by centrifugation, washed sequentially with H_2O and acetone several times，and dried at 100 ℃ for 12 h. The product was obtained as a light-yellow solid (103 mg, 78% yield).

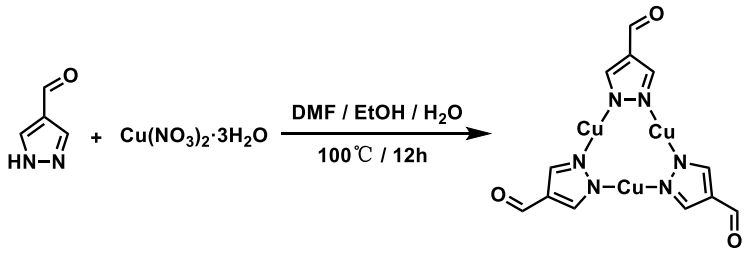

Figure S7. Schematic illustration of the synthesis of $Cu_3(PyCA)_3$.

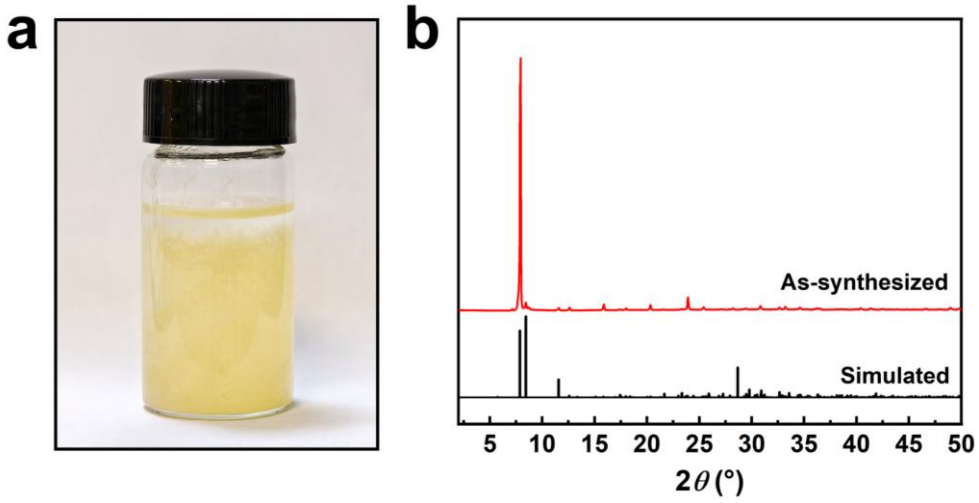

Figure S8. Photograph of the as-synthesized $Cu_3(PyCA)_3$ before sonication (a). Powder X-ray diffraction (PXRD) pattern of as-synthesized $Cu_3(PyCA)_3$ (b) and the along with simulated pattern from CCDC 2026064.[19]

3.3 Synthesis of Pd-PCOF-1(Cu_3)

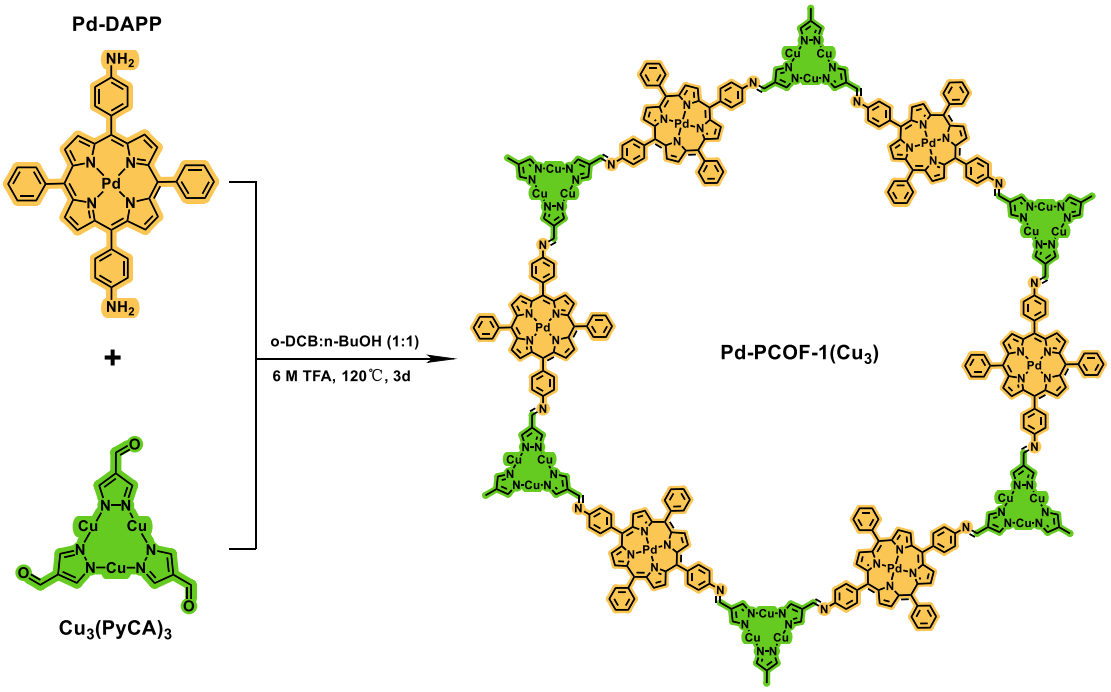

Figure S9. Schematic illustration of the synthesis of Pd-PCOF-1(Cu_3).

3.4 Synthesis of Pd-PCOF-2(Cu_3) and PCOF-2(Cu_3)

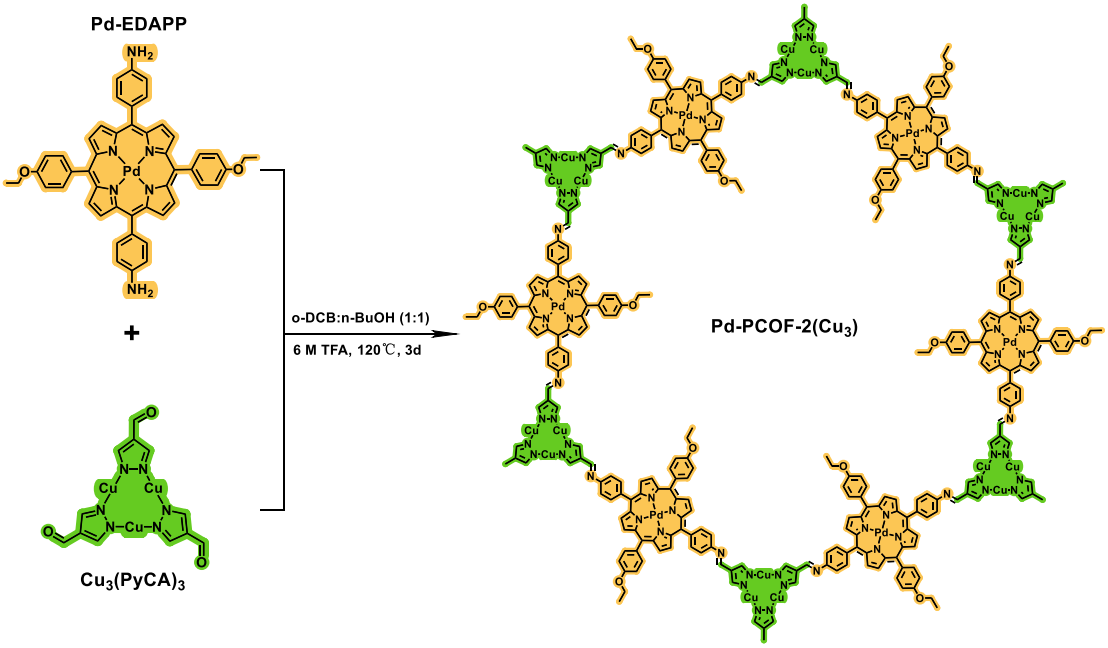

Figure S10. Schematic illustration of the synthesis of Pd-PCOF-2(Cu_3).

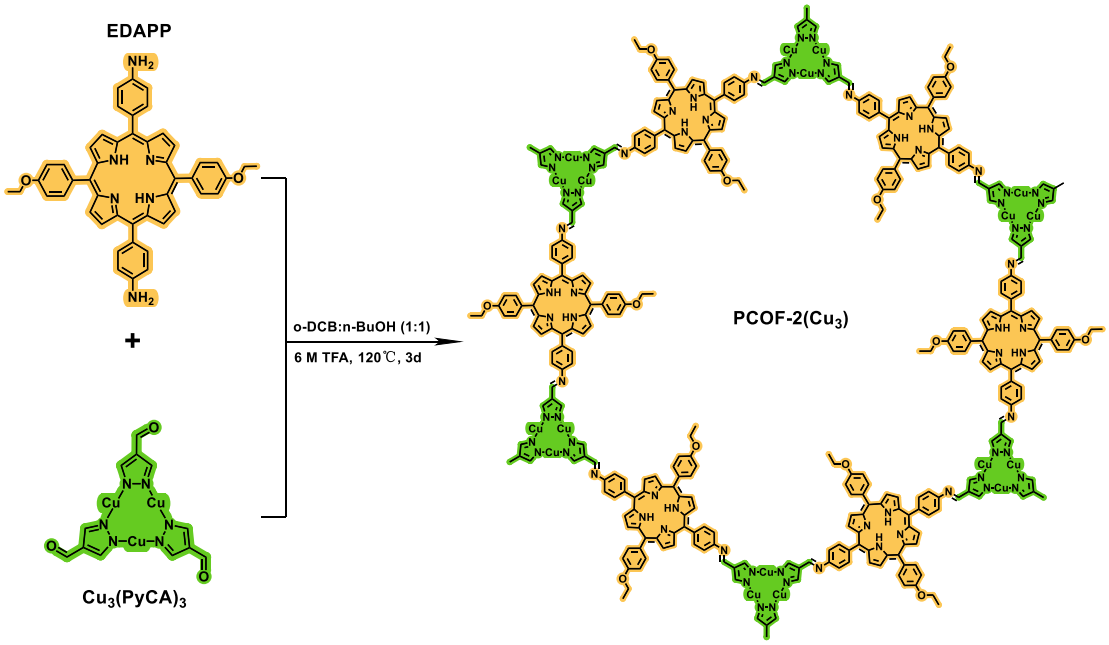

Figure S11. Schematic illustration of the synthesis of PCOF-2(Cu_3).

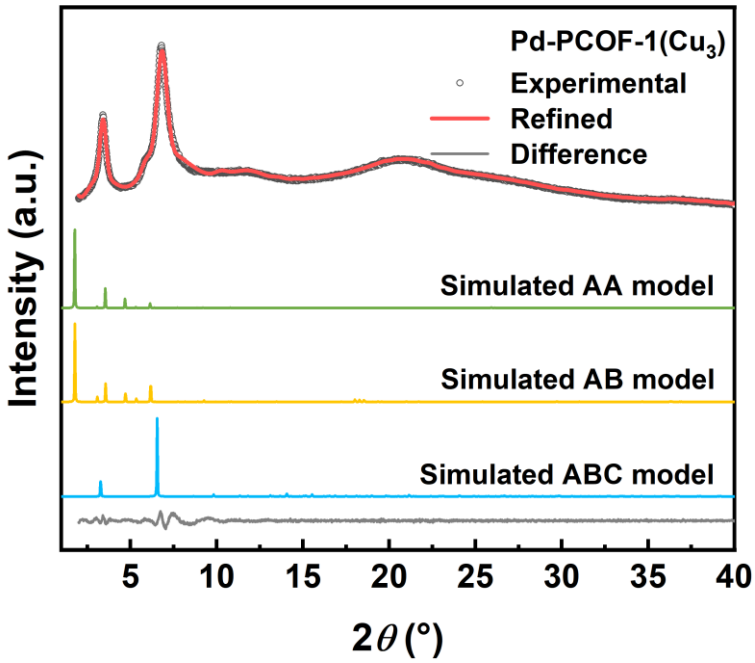

Figure S12. PXRD patterns of Pd-PCOF-1(Cu_3) with the experimental profiles, Pawley refined, difference curve, and simulated profiles of AA, AB, and ABC models.

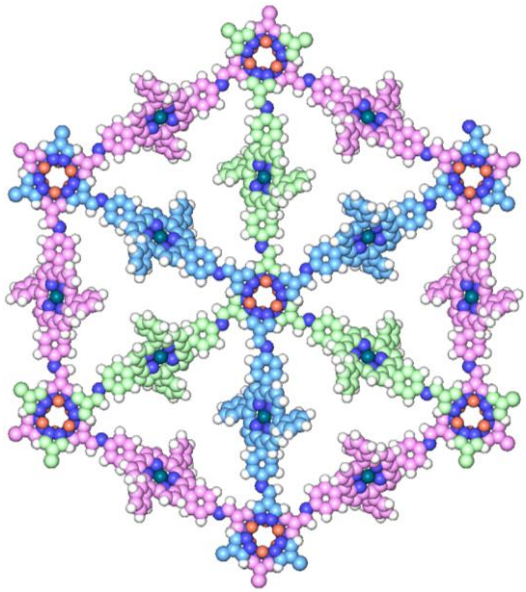

Figure S13. ABC stacking model of Pd-PCOF-1(Cu_3) viewed from *c* axis. The dark green, orange, dark blue and white spheres refer to palladium, copper, nitrogen and hydrogen, respectively.

Table S2. Fractional atomic coordinates for Pd-PCOF-1(Cu_3)-AA.

Pd-PCOF-1(Cu_3)-AA

Space group symmetry: *P*6/*m*

***a* = *b* = 57.593 Å, *c* = 3.439 Å**

$\alpha = \beta = 90.00°$, $\gamma = 120.00°$

Number	Atom	x	y	z
1	C	13.964	29.208	1.719
2	C	12.75	28.896	1.719
3	C	12.602	27.486	1.719
4	N	13.895	26.948	1.719
5	C	14.778	28.039	1.719
6	C	18.566	25.334	1.719
7	C	18.248	26.593	1.719
8	C	16.906	26.736	1.719
9	N	16.376	25.45	1.719
10	C	17.455	24.577	1.719
11	C	16.227	28.108	1.719
12	C	17.524	23.026	1.719
13	C	18.981	22.165	1.719
14	C	17.083	29.532	1.719
15	C	18.53	29.667	1.719
16	C	19.263	30.864	1.719
17	C	18.631	32.073	1.719
18	C	17.266	32.081	1.719
19	C	16.538	30.881	1.719
20	C	19.141	20.722	1.719
21	C	20.355	20.013	1.719
22	C	21.564	20.676	1.719
23	C	21.526	22.044	1.719
24	C	20.31	22.742	1.719
25	C	24.854	16.933	1.719
26	N	26.201	16.882	1.719
27	N	26.664	18.127	1.719
28	C	25.612	18.968	1.719
29	C	24.448	18.241	1.719
30	C	23.07	18.739	1.719
31	N	22.843	20.018	1.719
32	Cu	28.386	19.05	1.719
33	H	14.092	30.219	1.719

34	H	12.138	29.711	1.719
35	H	19.572	25.186	1.719
36	H	19.076	27.184	1.719
37	H	19.296	28.986	1.719
38	H	20.349	30.855	1.719
39	H	16.761	33.043	1.719
40	H	15.582	31.254	1.719
41	H	18.463	19.951	1.719
42	H	20.328	18.931	1.719
43	H	22.469	22.585	1.719
44	H	20.64	23.714	1.719
45	H	24.212	16.062	1.719
46	H	25.695	20.047	1.719
47	H	22.268	18.016	1.719
48	H	19.194	32.997	1.719
49	Pd	43.194	24.938	1.719

Table S3. Fractional atomic coordinates for Pd-PCOF-1(Cu_3)-AB.

Pd-PCOF-1(Cu_3)-AB

Space group symmetry: *P*63/*m*

***a* = *b* = 57.297 Å, *c* = 4.949 Å**

$\alpha = \beta = 90.00°$, $\gamma = 120.00°$

Number	Atom	x	y	z
1	C	42.539	12.43	1.237
2	C	41.284	12.105	1.237
3	C	41.133	10.767	1.237
4	N	42.438	10.248	1.237
5	C	43.323	11.338	1.237
6	C	47.088	8.672	1.237
7	C	46.783	9.941	1.237
8	C	45.446	10.123	1.237
9	N	44.906	8.75	1.237
10	C	45.995	7.877	1.237
11	C	44.786	11.423	1.237
12	C	46.06	6.413	1.237
13	C	47.42	5.614	1.237
14	C	45.573	12.782	1.237
15	C	47.022	12.95	1.237
16	C	47.739	14.157	1.237
17	C	47.094	15.356	1.237
18	C	45.734	15.348	1.237
19	C	45.019	14.137	1.237
20	C	47.601	4.163	1.237
21	C	48.814	3.443	1.237
22	C	50.026	4.093	1.237
23	C	49.991	5.458	1.237
24	C	48.774	6.165	1.237
25	C	53.315	0.339	1.237
26	N	54.664	0.281	1.237
27	N	55.131	1.523	1.237
28	C	54.077	2.367	1.237
29	C	52.911	1.647	1.237
30	C	51.532	2.149	1.237
31	N	51.305	3.429	1.237
32	Cu	-0.396	2.389	1.237
33	C	43.335	4.096	1.237

34	C	44.592	4.422	1.237
35	C	44.744	5.761	1.237
36	N	43.439	6.28	1.237
37	C	42.552	5.19	1.237
38	C	38.79	7.862	1.237
39	C	39.093	6.593	1.237
40	C	40.429	6.41	1.237
41	N	40.972	7.78	1.237
42	C	39.884	8.654	1.237
43	C	41.086	5.109	1.237
44	C	39.818	10.116	1.237
45	C	38.459	10.915	1.237
46	C	40.291	3.756	1.237
47	C	38.839	3.592	1.237
48	C	38.116	2.388	1.237
49	C	38.757	1.189	1.237
50	C	40.118	1.194	1.237
51	C	40.839	2.4	1.237
52	C	38.28	12.366	1.237
53	C	37.07	13.088	1.237
54	C	35.858	12.439	1.237
55	C	35.889	11.075	1.237
56	C	37.104	10.366	1.237
57	C	32.589	16.205	1.237
58	N	31.243	16.266	1.237
59	N	30.771	15.024	1.237
60	C	31.818	14.175	1.237
61	C	32.987	14.894	1.237
62	C	34.363	14.387	1.237
63	N	34.583	13.107	1.237
64	Cu	29.042	14.114	1.237
65	Pd	14.336	8.302	1.237
66	H	42.652	13.435	1.237
67	H	40.705	12.937	1.237
68	H	48.093	8.554	1.237
69	H	47.63	10.51	1.237
70	H	47.821	12.308	1.237
71	H	48.826	14.166	1.237
72	H	45.224	16.31	1.237
73	H	44.073	14.549	1.237
74	H	46.963	3.358	1.237
75	H	48.791	2.358	1.237

76	H	50.944	5.986	1.237
77	H	49.177	7.111	1.237
78	H	24.018	49.093	1.237
79	H	54.16	3.446	1.237
80	H	50.729	1.428	1.237
81	H	43.222	3.089	1.237
82	H	45.173	3.591	1.237
83	H	37.786	7.982	1.237
84	H	38.246	6.028	1.237
85	H	38.039	4.233	1.237
86	H	37.028	2.38	1.237
87	H	40.627	0.233	1.237
88	H	41.785	1.992	1.237
89	H	38.917	13.172	1.237
90	H	37.095	14.172	1.237
91	H	34.935	10.55	1.237
92	H	36.697	9.421	1.237
93	H	33.238	17.072	1.237
94	H	31.726	13.097	1.237
95	H	35.168	15.106	1.237
96	H	47.643	16.288	1.237
97	H	38.2	0.261	1.237

Table S4. Fractional atomic coordinates for Pd-PCOF-1(Cu_3)-ABC.

Pd-PCOF-1(Cu_3)-ABC

Space group symmetry: *R*-3

***a* = *b* = 54.020 Å, *c* = 6.739 Å**

***α* = *β* = 90.00 °, *γ* = 120.00 °**

Number	Atom	x	y	z
1	C	-11.896	36.064	-0.362
2	C	-10.851	36.212	0.492
3	C	-11.231	37.146	1.443
4	N	-12.467	37.628	1.149
5	C	-12.888	36.948	0.044
6	C	-16.971	39.175	-0.122
7	C	-16.306	38.212	-0.823
8	C	-15.149	37.92	-0.121
9	N	-15.091	38.744	1.038
10	C	-16.227	39.479	1.016
11	C	-14.169	37.015	-0.555
12	C	-16.581	40.479	1.94
13	C	-17.786	41.19	1.73
14	C	-14.514	36.114	-1.598
15	C	-13.76	36.039	-2.784
16	C	-14.118	35.148	-3.801
17	C	-15.248	34.341	-3.662
18	C	-16.017	34.415	-2.5
19	C	-15.655	35.292	-1.473
20	C	-17.761	42.575	1.487
21	C	-18.948	43.285	1.293
22	C	-20.19	42.618	1.338
23	C	-20.211	41.236	1.562
24	C	-19.025	40.526	1.756
25	C	-23.338	46.439	1.288
26	N	-24.645	46.512	1.595
27	N	-25.149	45.289	1.61
28	C	-24.171	44.414	1.322
29	C	-23.005	45.115	1.097
30	C	-21.645	44.571	1.041
31	N	-21.451	43.3	1.228
32	Cu	27.267	44.778	2.594
33	H	-11.918	35.342	-1.164

34	H	-9.922	35.661	0.429
35	H	-17.886	39.641	-0.459
36	H	-16.618	37.816	-1.78
37	H	-12.9	36.674	-2.924
38	H	-13.52	35.08	-4.698
39	H	-16.892	33.787	-2.39
40	H	-16.257	35.318	-0.572
41	H	-16.816	43.106	1.443
42	H	-18.877	44.348	1.122
43	H	-21.157	40.711	1.607
44	H	-19.073	39.461	1.949
45	H	4.365	0.483	1.376
46	H	-24.265	43.341	1.432
47	H	-20.823	45.263	0.932
48	H	-15.526	33.658	-4.454
49	Pd	13.505	38.986	2.246

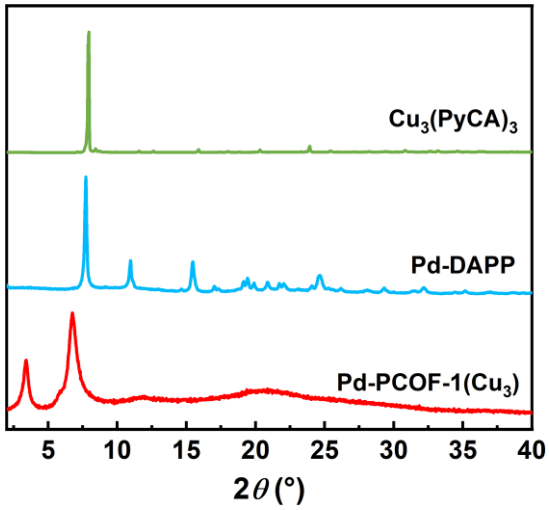

Figure S14. PXRD patterns of Pd-PCOF-1(Cu_3), $Cu_3(PyCA)_3$ and Pd-DAPP.

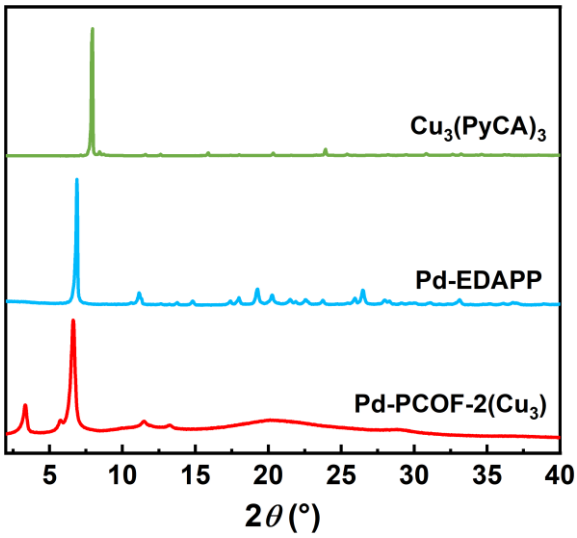

Figure S15. PXRD patterns of Pd-PCOF-2(Cu_3), $Cu_3(PyCA)_3$ and Pd-EDAPP.

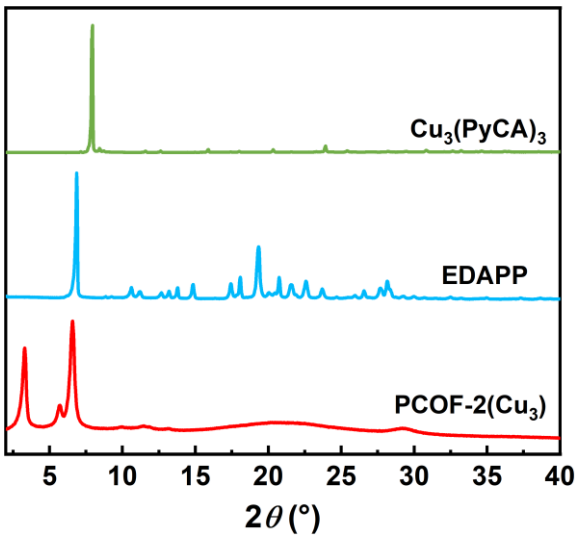

Figure S16. PXRD patterns of PCOF-2(Cu_3), $Cu_3(PyCA)_3$ and EDAPP.

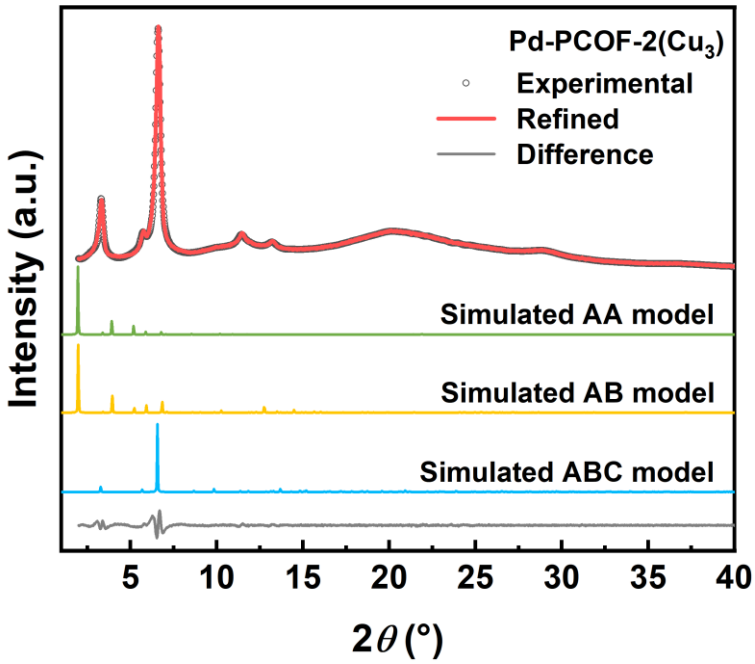

Figure S17. PXRD patterns of Pd-PCOF-2(Cu_3) with the experimental profiles, Pawley refined, difference curve, and simulated profiles of AA, AB, and ABC models.

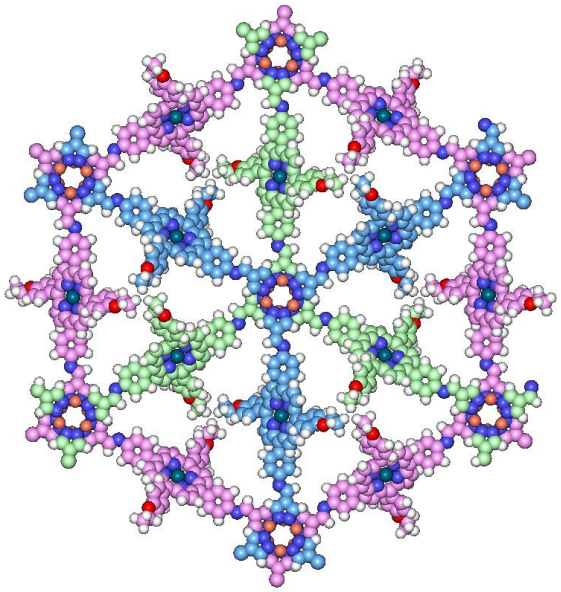

Figure S18. ABC stacking model of Pd-PCOF-2(Cu_3) viewed from *c* axis. The dark green, orange, dark blue, red and white spheres refer to palladium, copper, nitrogen, oxygen and hydrogen, respectively.

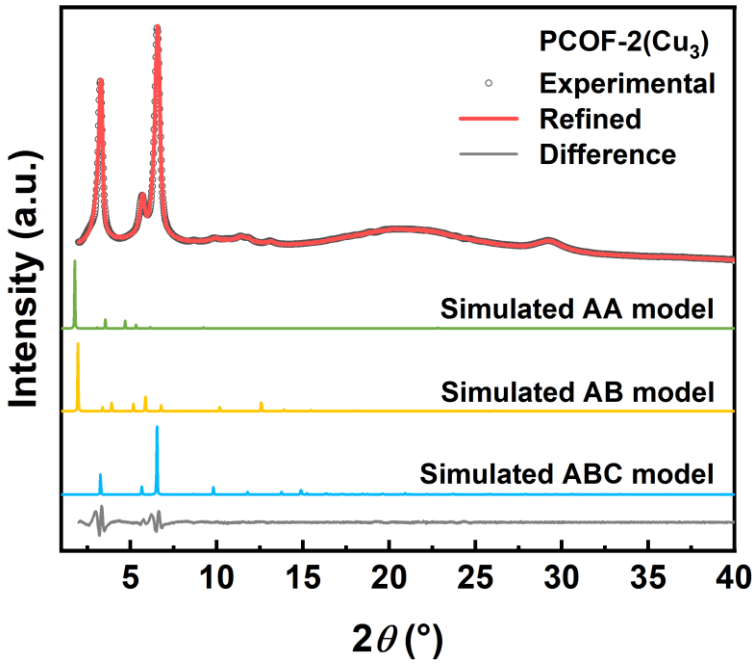

Figure S19. PXRD patterns of PCOF-2(Cu_3) with the experimental profiles, Pawley refined, difference curve, and simulated profiles of AA, AB, and ABC models.

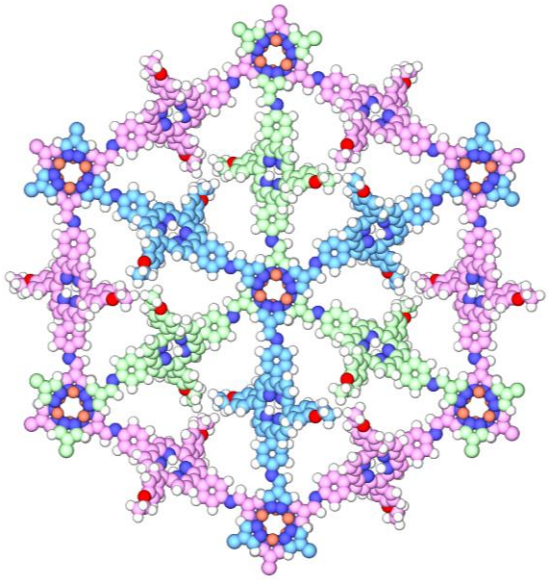

Figure S20. ABC stacking model of PCOF-2(Cu_3) viewed from *c* axis. The orange, dark blue, red and white spheres refer to copper, nitrogen, oxygen and hydrogen, respectively.

Table S5. Fractional atomic coordinates for Pd-PCOF-2(Cu_3)-AA.

Pd-PCOF-2(Cu_3)-AA

Space group symmetry: *P*3

***a* = *b* = 52.094 Å, *c* = 4.277 Å**

***α* = *β* = 90.00 °, *γ* = 120.00 °**

Number	Atom	x	y	z
1	C	-14.113	40.65	1.561
2	C	-15.269	40.306	1.054
3	C	-15.251	38.854	0.869
4	N	-14.058	38.369	1.297
5	C	-13.321	39.427	1.715
6	C	-9.541	36.855	2.668
7	C	-9.971	38.14	2.826
8	C	-11.255	38.203	2.309
9	N	-11.641	36.971	1.903
10	C	-10.576	36.15	2.074
11	C	-11.987	39.397	2.166
12	C	-12.87	32.254	0.83
13	C	-11.622	32.613	1.015
14	C	-11.618	34.057	1.27
15	N	-12.884	34.522	1.172
16	C	-13.691	33.455	0.981
17	C	-10.497	34.791	1.703
18	C	-17.253	35.959	-0.442
19	C	-16.911	34.649	-0.269
20	C	-15.742	34.627	0.47
21	N	-15.291	35.895	0.615
22	C	-16.256	36.715	0.148
23	C	-16.321	38.107	0.333
24	C	-15.1	33.478	0.982
25	C	-9.192	34.077	1.887
26	C	-11.274	40.696	2.401
27	C	-17.644	38.785	0.135
28	C	-15.869	32.294	1.587
29	C	-10.085	40.988	1.708
30	C	-9.408	42.19	1.926
31	C	-9.923	43.147	2.806
32	C	-11.124	42.871	3.486
33	C	-11.773	41.648	3.302

34	C	-9.106	32.973	2.747
35	C	-7.876	32.386	3.041
36	C	-6.692	32.909	2.494
37	C	-6.771	33.994	1.614
38	C	-8.011	34.558	1.293
39	C	-17.267	32.096	1.454
40	C	-17.915	31.003	2.038
41	C	-17.218	30.084	2.818
42	C	-15.851	30.309	3.048
43	C	-15.209	31.407	2.473
44	C	-17.785	39.918	-0.682
45	C	-18.979	40.647	-0.696
46	C	-20.071	40.227	0.085
47	C	-19.972	39.035	0.805
48	C	-18.768	38.332	0.846
49	C	-3.454	29.759	4.518
50	N	-2.326	29.944	5.226
51	N	-2.01	31.228	5.208
52	C	-2.924	31.893	4.479
53	C	-3.861	30.983	4.025
54	C	-5.143	31.274	3.378
55	N	-5.403	32.47	2.948
56	Cu	-0.588	32.028	6.282
57	C	-22.624	44.334	0.913
58	N	-23.797	44.529	1.541
59	N	-24.466	43.389	1.565
60	C	-23.732	42.438	0.964
61	C	-22.547	43.008	0.536
62	C	-21.334	42.305	0.108
63	N	-21.256	41.017	0.254
64	Cu	26.008	43.077	2.607
65	O	-9.239	44.308	2.968
66	O	34.149	29.01	3.37
67	C	34.874	27.974	4.037
68	C	33.901	26.908	4.514
69	C	16.382	0.283	3.7
70	C	17.425	1.386	3.622
71	Pd	12.248	38.559	1.26
72	H	-13.834	41.671	1.77
73	H	-16.059	41.011	0.844
74	H	-8.566	36.498	2.957
75	H	-9.385	38.937	3.26

76	H	-13.198	31.245	0.619
77	H	-10.784	31.932	0.989
78	H	-18.141	36.309	-0.944
79	H	-17.429	33.827	-0.732
80	H	-9.682	40.284	0.993
81	H	-8.491	42.391	1.387
82	H	-11.553	43.583	4.179
83	H	-12.68	41.454	3.846
84	H	-9.991	32.585	3.218
85	H	-7.85	31.578	3.76
86	H	-5.868	34.419	1.196
87	H	-8.043	35.409	0.63
88	H	-17.922	32.786	0.974
89	H	-18.982	30.881	1.897
90	H	-15.272	29.669	3.697
91	H	-14.194	31.574	2.782
92	H	-16.949	40.278	-1.256
93	H	-19.038	41.54	-1.304
94	H	-20.807	38.693	1.404
95	H	-18.703	37.455	1.472
96	H	-3.976	28.816	4.43
97	H	-2.953	32.968	4.365
98	H	-5.884	30.487	3.322
99	H	-21.831	45.068	0.858
100	H	-23.991	41.388	0.943
101	H	-20.461	42.892	-0.149
102	H	35.404	28.381	4.923
103	H	35.605	27.509	3.339
104	H	34.456	26.102	5.038
105	H	33.361	26.472	3.647
106	H	33.166	27.354	5.217
107	H	16.241	-0.003	4.763
108	H	15.421	0.662	3.288
109	H	18.388	1.028	4.043
110	H	17.083	2.267	4.205
111	H	17.578	1.691	2.565

Table S6. Fractional atomic coordinates for Pd-PCOF-2(Cu_3)-AB.

Pd-PCOF-2(Cu_3)-AB

Space group symmetry: *P*63

***a* = *b* = 51.712 Å, *c* = 7.301 Å**

***α* = *β* = 90.00 °, *γ* = 120.00 °**

Number	Atom	x	y	z
1	C	38.821	11.688	1.708
2	C	37.536	11.411	1.573
3	C	37.408	9.953	1.604
4	N	38.638	9.414	1.706
5	C	39.53	10.411	1.861
6	C	42.998	8.062	0.048
7	C	42.805	9.256	0.706
8	C	41.552	9.196	1.303
9	N	40.966	8.03	0.957
10	C	41.842	7.315	0.221
11	C	40.923	10.233	2.039
12	C	39.168	3.444	0.318
13	C	40.262	3.843	-0.305
14	C	40.506	5.227	0.101
15	N	39.513	5.615	0.923
16	C	38.717	4.552	1.169
17	C	41.637	5.997	-0.248
18	C	34.99	7.093	2.025
19	C	35.38	5.779	2.147
20	C	36.756	5.746	1.971
21	N	37.194	6.994	1.711
22	C	36.137	7.83	1.763
23	C	36.193	9.237	1.647
24	C	37.565	4.583	1.992
25	C	42.754	5.302	-0.941
26	C	41.729	11.205	2.899
27	C	34.93	10.011	1.781
28	C	37.162	3.406	2.872
29	C	43.113	11.03	3.144
30	C	43.879	12.047	3.723
31	C	43.278	13.237	4.133
32	C	41.879	13.314	4.138
33	C	41.118	12.286	3.58

34	C	43.373	4.212	-0.312
35	C	44.446	3.564	-0.916
36	C	44.945	4.011	-2.15
37	C	44.346	5.114	-2.775
38	C	43.239	5.743	-2.186
39	C	36.334	3.621	4.002
40	C	35.795	2.552	4.722
41	C	36.107	1.24	4.373
42	C	37.114	1.019	3.425
43	C	37.646	2.087	2.698
44	C	34.735	10.831	2.904
45	C	33.527	11.502	3.087
46	C	32.479	11.343	2.165
47	C	32.665	10.514	1.05
48	C	33.891	9.868	0.846
49	C	48.06	0.305	-2.618
50	N	49.359	0.247	-2.277
51	N	49.859	1.47	-2.284
52	C	48.89	2.336	-2.634
53	C	47.72	1.625	-2.838
54	C	46.362	2.159	-2.694
55	N	46.148	3.44	-2.682
56	Cu	51.439	1.985	-1.266
57	C	29.403	14.848	3.774
58	N	28.198	14.809	4.37
59	N	27.74	13.569	4.336
60	C	28.636	12.79	3.703
61	C	29.712	13.577	3.335
62	C	31.031	13.118	2.892
63	N	31.191	11.921	2.415
64	Cu	26.236	12.924	5.406
65	O	44.066	14.279	4.505
66	O	35.454	0.189	5.036
67	C	35.099	-0.953	4.247
68	C	33.642	-1.306	4.493
69	C	43.666	15.602	4.538
70	C	44.843	16.486	4.913
71	H	39.249	12.678	1.624
72	H	36.754	12.14	1.408
73	H	43.887	7.789	-0.505
74	H	43.484	10.097	0.672
75	H	38.632	2.543	0.057

76	H	40.787	3.278	-1.065
77	H	33.979	7.458	2.14
78	H	34.714	4.945	2.319
79	H	43.624	10.113	2.901
80	H	44.951	11.924	3.807
81	H	41.367	14.166	4.562
82	H	40.053	12.361	3.706
83	H	43.034	3.873	0.66
84	H	44.924	2.745	-0.394
85	H	44.737	5.486	-3.713
86	H	42.779	6.589	-2.682
87	H	36.077	4.619	4.328
88	H	35.096	2.746	5.525
89	H	37.479	0.017	3.237
90	H	38.442	1.837	2.032
91	H	35.513	10.931	3.651
92	H	33.39	12.103	3.977
93	H	31.858	10.367	0.343
94	H	34.019	9.229	-0.019
95	H	47.368	-0.518	-2.493
96	H	48.973	3.408	-2.517
97	H	45.573	1.47	-2.41
98	H	30.05	15.715	3.758
99	H	28.571	11.712	3.639
100	H	31.882	13.776	3.028
101	H	35.736	-1.812	4.535
102	H	35.231	-0.785	3.162
103	H	33.367	-2.201	3.895
104	H	32.992	-0.457	4.192
105	H	33.476	-1.527	5.567
106	H	43.294	15.905	3.535
107	H	42.86	15.75	5.288
108	H	45.715	16.268	4.261
109	H	45.123	16.308	5.969
110	H	44.562	17.554	4.798
111	Pd	39.085	82.06	5.007

Table S7. Fractional atomic coordinates for Pd-PCOF-2(Cu_3)-ABC.

Pd-PCOF-2(Cu_3)-ABC

Space group symmetry: *R*-3

***a* = *b* = 53.903 Å, *c* = 6.953 Å**

***α* = *β* = 90.00 °, *γ* = 120.00 °**

Number	Atom	x	y	z
1	C	-11.797	35.935	-0.191
2	C	-10.765	36.118	0.671
3	C	-11.166	37.078	1.586
4	N	-12.401	37.541	1.26
5	C	-12.795	36.835	0.16
6	C	-16.883	39.049	-0.136
7	C	-16.177	38.115	-0.833
8	C	-15.047	37.812	-0.091
9	N	-15.04	38.617	1.086
10	C	-16.183	39.34	1.032
11	C	-14.048	36.912	-0.498
12	C	-16.568	40.347	1.936
13	C	-17.772	41.048	1.688
14	C	-14.329	36.051	-1.599
15	C	-13.457	35.962	-2.699
16	C	-13.73	35.102	-3.764
17	C	-14.907	34.354	-3.792
18	C	-15.805	34.453	-2.712
19	C	-15.511	35.281	-1.625
20	C	-17.75	42.429	1.425
21	C	-18.939	43.134	1.221
22	C	-20.18	42.467	1.273
23	C	-20.197	41.085	1.499
24	C	-19.008	40.379	1.703
25	C	-23.305	46.302	1.314
26	N	-24.599	46.385	1.669
27	N	-25.115	45.166	1.688
28	C	-24.157	44.284	1.356
29	C	-22.991	44.977	1.1
30	C	-21.637	44.422	1
31	N	-21.443	43.15	1.184
32	Cu	27.184	44.669	2.681
33	O	-15.133	33.558	-4.868

34	C	16.289	-1.726	9.745
35	C	16.159	-0.972	11.057
36	H	-11.804	35.176	-0.959
37	H	-9.835	35.567	0.64
38	H	-17.787	39.517	-0.5
39	H	-16.446	37.749	-1.815
40	H	-12.56	36.557	-2.732
41	H	-13.025	35.019	-4.578
42	H	-16.725	33.883	-2.695
43	H	-16.204	35.31	-0.792
44	H	-16.808	42.963	1.383
45	H	-18.869	44.197	1.045
46	H	-21.141	40.557	1.546
47	H	-19.054	39.315	1.903
48	H	-22.603	47.123	1.382
49	H	-24.261	43.211	1.45
50	H	-20.815	45.111	0.874
51	H	16.461	-0.994	8.925
52	H	17.149	-2.426	9.814
53	H	15.388	-0.178	10.964
54	H	17.134	-0.51	11.315
55	H	15.869	-1.664	11.872
56	Pd	13.476	38.901	2.318

Table S8. Fractional atomic coordinates for PCOF-2(Cu_3)-AA.

PCOF-2(Cu_3)-AA

Space group symmetry: *P*3

***a* = *b* = 51.514 Å, *c* = 4.333 Å**

***α* = *β* = 90.00 °, *γ* = 120.00 °**

Number	Atom	x	y	z
1	C	-13.912	41.347	0.804
2	C	-15.146	40.907	0.891
3	C	-15.128	39.758	1.797
4	N	-13.855	39.494	2.177
5	C	-13.096	40.472	1.635
6	C	-9.464	38.343	-0.016
7	C	-9.829	39.603	0.374
8	C	-10.955	39.476	1.167
9	N	-11.304	38.168	1.246
10	C	-10.377	37.468	0.549
11	C	-11.696	40.555	1.708
12	C	-12.504	33.285	0.914
13	C	-11.278	33.726	0.766
14	C	-11.347	35.188	0.758
15	N	-12.626	35.579	0.962
16	C	-13.369	34.456	1.089
17	C	-10.263	36.058	0.491
18	C	-17.342	36.757	2.198
19	C	-16.913	35.477	1.989
20	C	-15.567	35.543	1.659
21	N	-15.172	36.842	1.689
22	C	-16.24	37.59	2.069
23	C	-16.252	39.012	2.216
24	C	-14.758	34.404	1.375
25	C	-8.915	35.475	0.195
26	C	-11.043	41.881	2.071
27	C	-17.439	39.715	2.864
28	C	-15.404	33.056	1.422
29	C	-9.647	41.986	2.267
30	C	-9.054	43.18	2.686
31	C	-9.834	44.294	2.991
32	C	-11.227	44.206	2.843
33	C	-11.819	43.021	2.398

34	C	-8.744	34.443	-0.745
35	C	-7.511	33.793	-0.872
36	C	-6.408	34.215	-0.107
37	C	-6.546	35.322	0.733
38	C	-7.789	35.93	0.905
39	C	-16.497	32.76	0.592
40	C	-17.118	31.511	0.654
41	C	-16.633	30.509	1.502
42	C	-15.519	30.796	2.321
43	C	-14.938	32.067	2.302
44	C	-17.814	41.051	2.575
45	C	-18.908	41.657	3.204
46	C	-19.672	40.947	4.139
47	C	-19.302	39.644	4.457
48	C	-18.173	39.066	3.88
49	C	-3.504	30.3	0.245
50	N	-2.29	30.172	0.811
51	N	-1.704	31.356	0.84
52	C	-2.535	32.269	0.309
53	C	-3.697	31.628	-0.08
54	C	-4.988	32.259	-0.373
55	N	-5.157	33.515	-0.094
56	Cu	-0.102	31.774	1.873
57	C	-22.373	44.483	6.329
58	N	-23.452	44.431	7.132
59	N	-23.918	43.194	7.147
60	C	-23.147	42.424	6.361
61	C	-22.149	43.217	5.825
62	C	-21.006	42.786	5.014
63	N	-20.796	41.52	4.823
64	Cu	26.071	42.603	8.212
65	O	-9.212	45.413	3.445
66	O	34.209	29.27	1.492
67	C	34.773	28.187	2.234
68	C	33.914	26.948	2.041
69	C	15.919	1.906	3.985
70	C	16.968	2.92	4.417
71	H	-13.573	42.153	0.169
72	H	-15.958	41.274	0.285
73	H	-8.62	38.099	-0.648
74	H	-9.331	40.509	0.075
75	H	-12.043	37.776	1.864

76	H	-12.773	32.238	0.916
77	H	-10.41	33.088	0.677
78	H	-18.375	37.026	2.363
79	H	-17.545	34.604	2.067
80	H	-14.236	37.211	1.445
81	H	-8.992	41.134	2.177
82	H	-7.981	43.221	2.828
83	H	-11.867	45.042	3.089
84	H	-12.896	43.01	2.368
85	H	-9.576	34.115	-1.351
86	H	-7.421	32.976	-1.575
87	H	-5.702	35.665	1.32
88	H	-7.878	36.731	1.629
89	H	-16.873	33.502	-0.101
90	H	-17.969	31.309	0.016
91	H	-15.108	30.064	3.002
92	H	-14.113	32.276	2.972
93	H	-17.293	41.662	1.872
94	H	-19.161	42.673	2.934
95	H	-19.852	39.096	5.213
96	H	-17.868	38.107	4.257
97	H	-4.252	29.518	0.225
98	H	-2.362	33.336	0.333
99	H	-5.828	31.626	-0.627
100	H	-21.768	45.366	6.168
101	H	-23.281	41.359	6.222
102	H	-20.296	43.531	4.679
103	H	34.796	28.434	3.317
104	H	35.802	27.97	1.871
105	H	34.352	26.096	2.604
106	H	33.866	26.682	0.964
107	H	32.885	27.137	2.417
108	H	15.252	2.375	3.229
109	H	15.321	1.602	4.872
110	H	17.713	2.437	5.087
111	H	16.479	3.757	4.961
112	H	17.493	3.322	3.524

Table S9. Fractional atomic coordinates for PCOF-2(Cu_3)-AB.

PCOF-2(Cu_3)-AB

Space group symmetry: *P*63

***a* = *b* = 51.309 Å, *c* = 7.323 Å**

***α* = *β* = 90.00 °, *γ* = 120.00 °**

Number	Atom	x	y	z
1	C	38.049	11.694	1.223
2	C	36.786	11.331	1.165
3	C	36.772	9.876	1.068
4	N	38.036	9.402	1.081
5	C	38.858	10.467	1.252
6	C	42.279	7.858	-0.301
7	C	41.958	9.178	-0.103
8	C	40.866	9.205	0.752
9	N	40.443	7.939	0.981
10	C	41.317	7.117	0.36
11	C	40.28	10.371	1.308
12	C	38.916	3.103	0.586
13	C	40.176	3.476	0.513
14	C	40.184	4.932	0.583
15	N	38.925	5.401	0.701
16	C	38.117	4.318	0.79
17	C	41.341	5.72	0.488
18	C	34.632	7.085	-0.163
19	C	34.95	5.749	-0.145
20	C	36.076	5.614	0.651
21	N	36.514	6.841	1.025
22	C	35.618	7.738	0.557
23	C	35.608	9.113	0.858
24	C	36.711	4.391	0.984
25	C	42.626	5.079	0.832
26	C	41.165	11.521	1.805
27	C	34.308	9.762	1.141
28	C	35.906	3.178	1.454
29	C	42.583	11.458	1.759
30	C	43.369	12.595	1.973
31	C	42.774	13.815	2.284
32	C	41.404	13.831	2.587
33	C	40.633	12.675	2.426

34	C	42.838	4.731	2.174
35	C	44.014	4.099	2.559
36	C	45.008	3.82	1.612
37	C	44.815	4.19	0.272
38	C	43.615	4.799	-0.124
39	C	34.492	3.13	1.412
40	C	33.793	1.952	1.694
41	C	34.468	0.796	2.076
42	C	35.847	0.882	2.323
43	C	36.535	2.074	2.077
44	C	33.997	10.055	2.477
45	C	32.808	10.704	2.798
46	C	31.894	11.044	1.792
47	C	32.183	10.724	0.457
48	C	33.401	10.112	0.127
49	C	47.72	0.316	3.717
50	N	48.956	0.269	4.242
51	N	49.494	1.476	4.197
52	C	48.623	2.323	3.621
53	C	47.488	1.608	3.291
54	C	46.233	2.137	2.772
55	N	46.227	3.193	2.018
56	Cu	51.053	1.992	5.232
57	C	29.158	14.556	3.869
58	N	27.984	14.567	4.521
59	N	27.453	13.356	4.476
60	C	28.268	12.549	3.774
61	C	29.367	13.286	3.371
62	C	30.625	12.771	2.83
63	N	30.656	11.672	2.141
64	Cu	25.925	12.789	5.559
65	O	43.559	14.953	2.284
66	O	33.736	-0.371	2.216
67	C	34.355	-1.612	2.418
68	C	33.303	-2.705	2.431
69	C	42.988	16.208	2.033
70	C	44.086	17.219	1.745
71	H	38.372	12.717	1.104
72	H	35.946	12.006	1.062
73	H	43.109	7.487	-0.887
74	H	42.472	10.023	-0.543
75	H	39.705	7.647	1.658

76	H	38.572	2.093	0.417
77	H	41.015	2.82	0.321
78	H	33.793	7.524	-0.685
79	H	34.43	4.976	-0.694
80	H	37.294	7.04	1.69
81	H	43.115	10.543	1.568
82	H	44.442	12.537	1.838
83	H	40.931	14.726	2.967
84	H	39.636	12.7	2.83
85	H	42.086	4.948	2.924
86	H	44.158	3.84	3.601
87	H	45.579	3.978	-0.464
88	H	43.456	5.042	-1.167
89	H	33.888	3.989	1.193
90	H	32.715	1.934	1.592
91	H	36.398	0.041	2.717
92	H	37.559	2.12	2.409
93	H	34.681	9.783	3.272
94	H	32.589	10.928	3.835
95	H	31.48	10.976	-0.327
96	H	33.637	9.915	-0.911
97	H	47.023	-0.512	3.7
98	H	48.766	3.394	3.541
99	H	45.307	1.634	3.028
100	H	29.844	15.391	3.828
101	H	28.133	11.48	3.672
102	H	31.544	13.299	3.063
103	H	34.884	-1.621	3.387
104	H	35.085	-1.817	1.609
105	H	33.795	-3.694	2.51
106	H	32.709	-2.676	1.494
107	H	32.626	-2.567	3.3
108	H	42.324	16.155	1.146
109	H	42.399	16.543	2.912
110	H	44.752	16.846	0.941
111	H	44.684	17.402	2.655
112	H	43.634	18.176	1.42

Table S10. Fractional atomic coordinates for PCOF-2(Cu_3)-ABC.

PCOF-2(Cu_3)-ABC

Space group symmetry: *R*-3

***a* = *b* = 53.903 Å, *c* = 6.953 Å**

***α* = *β* = 90.00 °, *γ* = 120.00 °**

Number	Atom	x	y	z
1	C	-12.001	35.972	-0.295
2	C	-10.926	36.122	0.527
3	C	-11.249	37.119	1.435
4	N	-12.468	37.634	1.141
5	C	-12.929	36.936	0.073
6	C	-16.822	39.554	-0.148
7	C	-16.137	38.624	-0.876
8	C	-15.111	38.113	-0.093
9	N	-15.12	38.765	1.184
10	C	-16.237	39.66	1.108
11	C	-14.193	37.132	-0.548
12	C	-16.624	40.631	2.068
13	C	-17.827	41.34	1.836
14	C	-14.564	36.345	-1.677
15	C	-13.698	36.168	-2.773
16	C	-14.071	35.374	-3.859
17	C	-15.332	34.781	-3.911
18	C	-16.222	34.976	-2.838
19	C	-15.838	35.742	-1.734
20	C	-17.819	42.734	1.646
21	C	-19.01	43.43	1.42
22	C	-20.237	42.739	1.361
23	C	-20.239	41.347	1.509
24	C	-19.049	40.651	1.734
25	C	-23.405	46.535	1.312
26	N	-24.704	46.604	1.652
27	N	-25.205	45.379	1.671
28	C	-24.233	44.507	1.353
29	C	-23.072	45.213	1.108
30	C	-21.71	44.673	1.037
31	N	-21.506	43.406	1.24
32	Cu	27.318	44.865	2.663
33	O	-15.647	34.033	-5

34	C	16.839	-2.12	9.805
35	C	16.796	-1.369	11.125
36	H	-12.079	35.209	-1.054
37	H	-10.023	35.53	0.473
38	H	-17.637	40.148	-0.543
39	H	-16.347	38.386	-1.911
40	H	-12.734	36.65	-2.795
41	H	-13.372	35.216	-4.668
42	H	-17.208	34.53	-2.839
43	H	-16.533	35.846	-0.909
44	H	-16.886	43.286	1.669
45	H	-18.954	44.502	1.314
46	H	-21.173	40.801	1.469
47	H	-19.084	39.575	1.86
48	H	-22.713	47.363	1.387
49	H	-24.324	43.433	1.456
50	H	-20.894	45.368	0.908
51	H	16.999	-1.389	8.982
52	H	17.679	-2.848	9.829
53	H	15.973	-0.624	11.109
54	H	17.762	-0.847	11.289
55	H	16.628	-2.075	11.962
56	H	-14.665	38.42	2.056

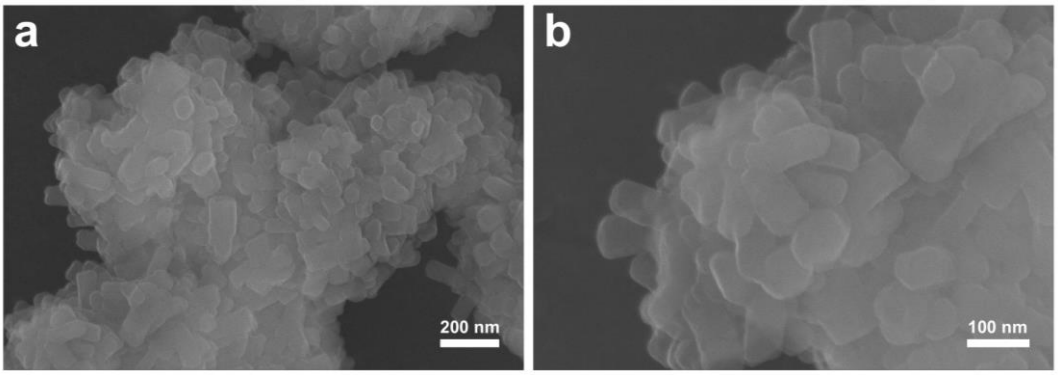

Figure S21. SEM images of Pd-PCOF-1(Cu_3).

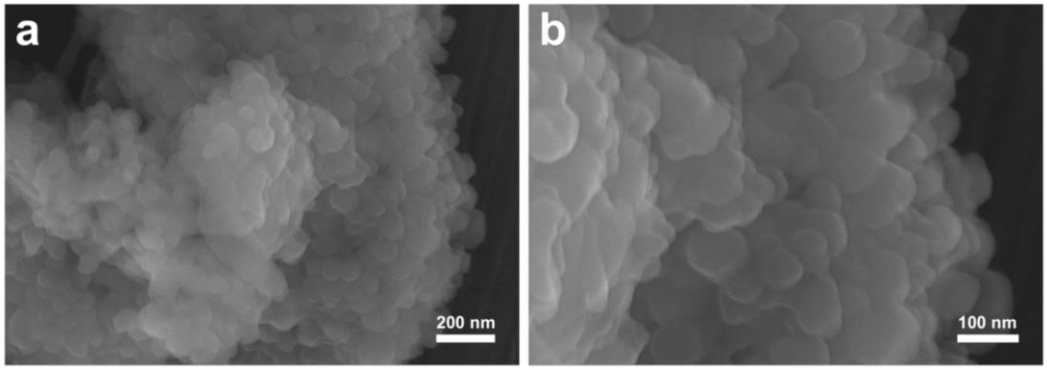

Figure S22. SEM images of Pd-PCOF-2(Cu_3).

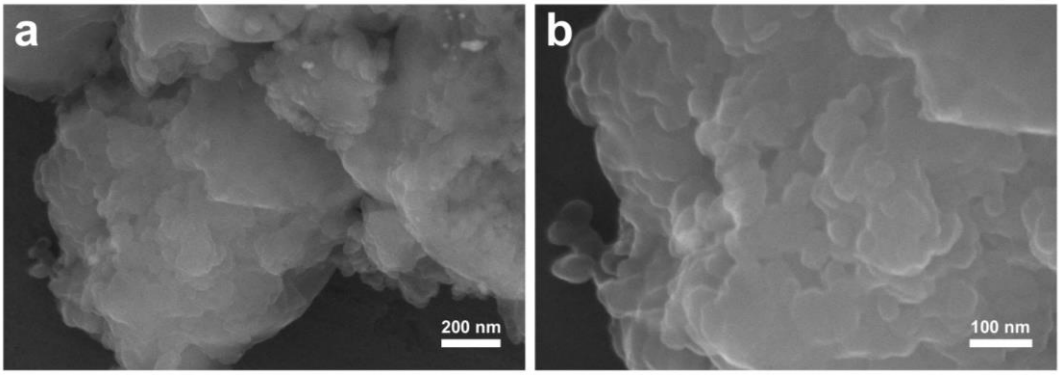

Figure S23. SEM images of PCOF-2(Cu_3).

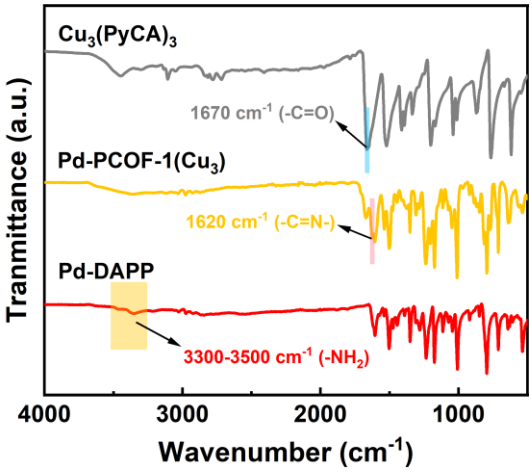

Figure S24. FT-IR spectra of Pd-PCOF-1(Cu_3), $Cu_3(PyCA)_3$ and Pd-DAPP.

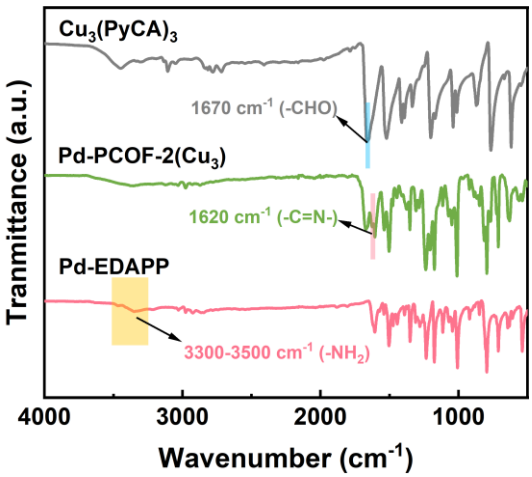

Figure S25. FT-IR spectra of Pd-PCOF-2(Cu_3), $Cu_3(PyCA)_3$ and Pd-EDAPP.

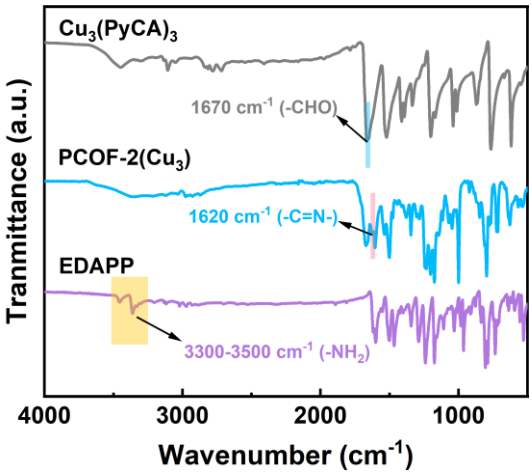

Figure S26. FT-IR spectra of PCOF-2(Cu_3), $Cu_3(PyCA)_3$ and EDAPP.

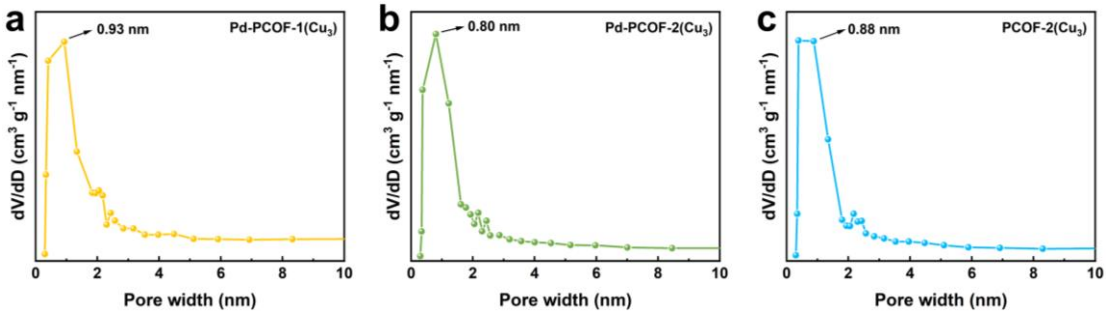

Figure S27. Pore size distribution profiles of Pd-PCOF-1(Cu_3) (a), Pd-PCOF-2(Cu_3) (b) and PCOF-2(Cu_3) (c) calculated by Nonlocal Density Functional Theory (NLDFT) modeling based on N_2 adsorption data.

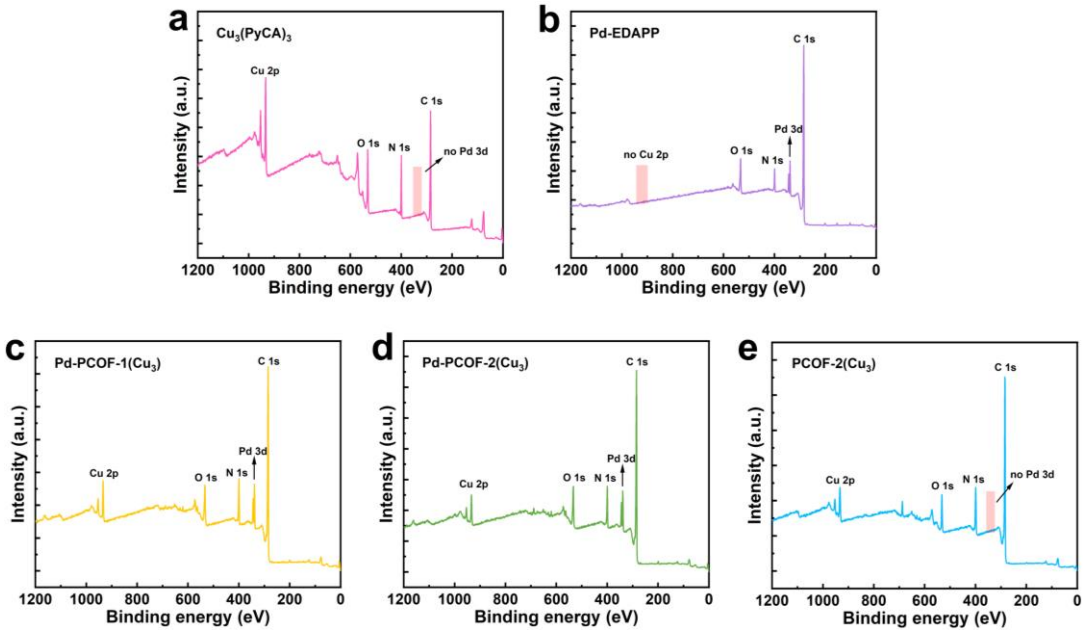

Figure S28. Survey scan XPS profiles of $Cu_3(PyCA)_3$ (a), Pd-EDAPP (b), Pd-PCOF-1(Cu_3) (c), Pd-PCOF-2(Cu_3) (d) and PCOF-2(Cu_3) (e).

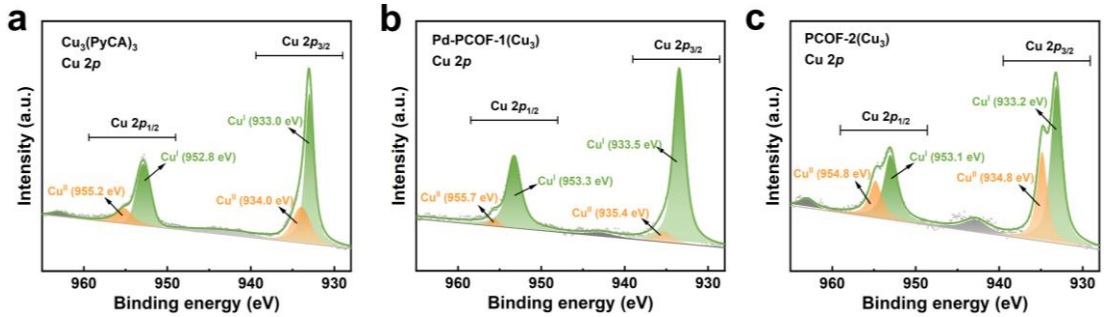

Figure S29. High-resolution Cu *2p* XPS profiles of $Cu_3(PyCA)_3$ (a), Pd-PCOF-1(Cu_3) (b), Pd-PCOF-2(Cu_3) (c) and PCOF-2(Cu_3) (d).

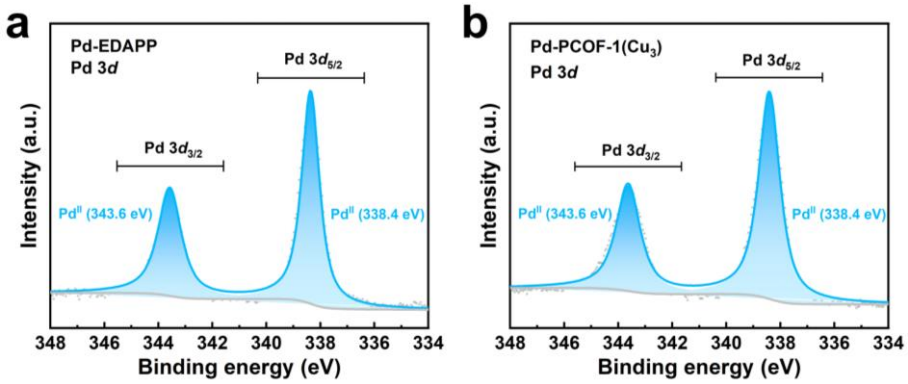

Figure S30. High-resolution Pd *3d* XPS profiles of Pd-EDAPP(a), Pd-PCOF-1(Cu_3) (b) and Pd-PCOF-2(Cu_3) (c).

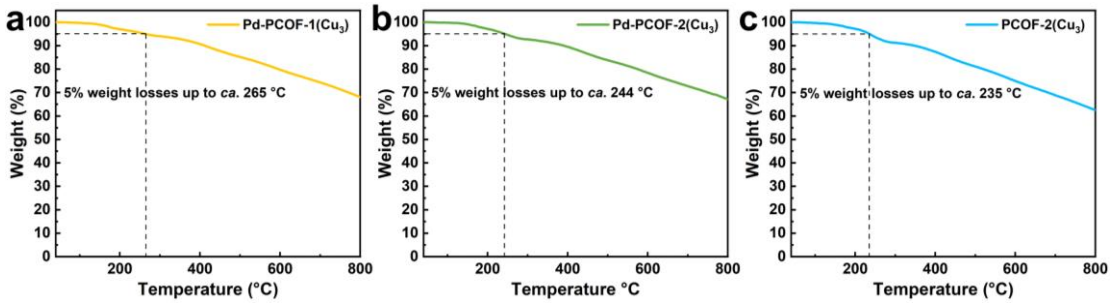

Figure S31. TGA curves of Pd-PCOF-1(Cu_3) (a), Pd-PCOF-2(Cu_3) (b) and PCOF-2(Cu_3) (c) under N_2 atmosphere.

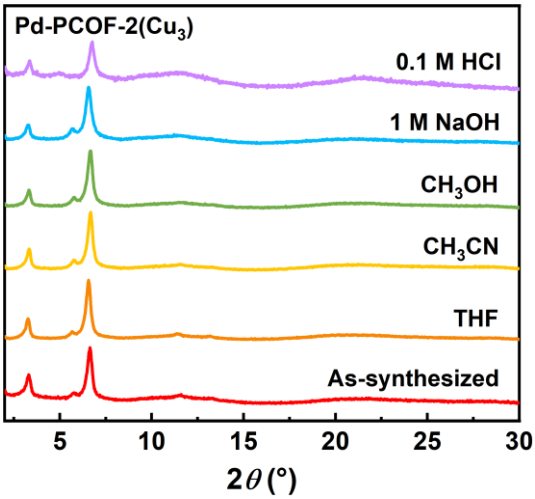

Figure S32. PXRD patterns of Pd-PCOF-2(Cu_3) after treatment with various solvents for 24 h.

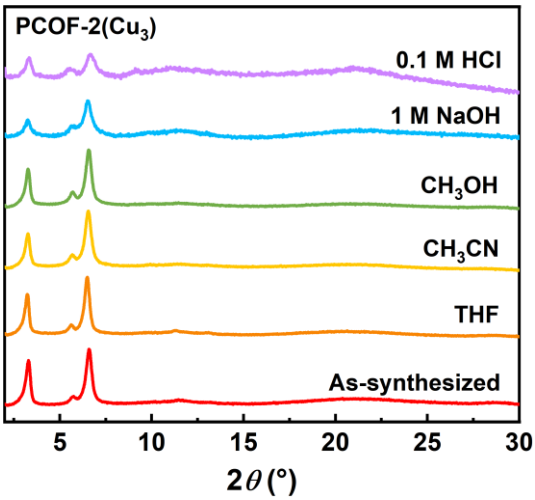

Figure S33. PXRD patterns of PCOF-2(Cu_3) after treatment with various solvents for 24 h.

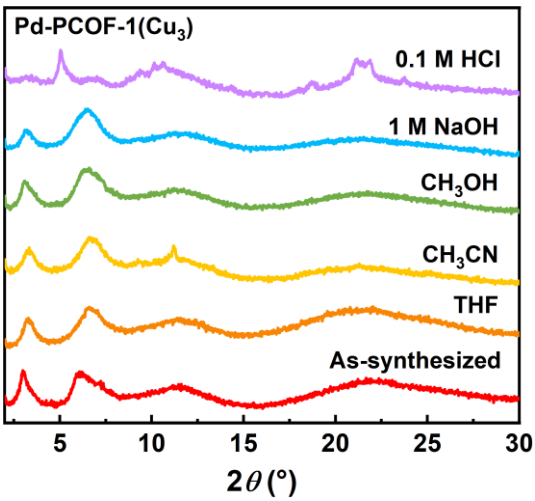

Figure S34. PXRD patterns of Pd-PCOF-1(Cu_3) after treatment with various solvents for 24 h.

4. Electrocatalytic performances

4.1 Determination of product

4.1.1 Determination of NH_3 by ^1H NMR measurement

After chronoamperometry test at a specific potential for 1000 s, 500 μL of the reaction electrolyte was collected and mixed with 500 μL of 2 mM maleic acid (dissolved in 1.5 M HCl) and 100 μL of DMSO-d_6. Subsequently, 600 μL of the mixture solution was used for ^1H NMR test on an NMR spectrometer (Bruker AVANCE III 400 MHz). The ammonia concentration was calculated by the corresponding standard curve, which was obtained by using a series of standard NH_4Cl solutions (2, 4, 6, 8 and 10 mM) in the same operation.

4.1.2 Determination of NH_3 by UV-Vis spectrophotometric measurement

The ammonia concentration can also be measured through the indophenol blue method. Firstly, solution A (1 M KOH containing 5 wt% salicylic acid and 5 wt% sodium citrate), solution B (50 mM NaClO) and solution C (1 wt% sodium nitroferricyanide solution) were prepared. Subsequently, 2 mL of the reaction electrolyte (diluted to a certain multiple) was mixed with 2 mL of solution A, 1 mL of solution B and 200 μL of solution C sequentially. After sitting for 2 h, the mixed solution was tested by UV-Vis spectrophotometer (UV-3600, Shimadzu) to obtain the absorption spectra (500 ~ 800 nm). According to the absorbance recorded at the wavelength of 655 nm, the ammonia concentration was calculated by the corresponding concentration-absorbance curve, which was obtained by using a series of standard NH_4Cl solutions (0, 0.1, 0.2, 0.3 and 0.4 mM) in the same operation.

4.1.3 Determination of NO_2^- by spectrophotometric measurement

The NO_2^- concentration was measured using the Griess test. Firstly, the Griess reagent was prepared by dissolving 400 mg of *p*-aminobenzene sulfonamide, 20 mg of N-(1-naphthyl) ethyldiamine dihydrochloride and 1 mL of phosphoric acid (85%) in 5 mL of deionized H_2O. Subsequently, 5 mL of the reaction electrolyte (diluted to a certain multiple) was mixed with 100 μL of the Griess reagent. After sitting for 0.5 h, the mixed solution was tested by UV-Vis spectrophotometer (UV-3600, Shimadzu) to obtain the absorption spectra (430 ~ 650 nm). According to the absorbance recorded at the wavelength of 540 nm, the ammonia concentration

was calculated by the corresponding concentration-absorbance curve, which was obtained by using a series of standard KNO_2 solutions (0, 2, 5, 10, 20, 30, 40 and 50 μM) in the same operation.

4.1.4 Determination of H_2 by gas chromatographic method

The H_2 product was collected and detected through on-line gas chromatograph (FULI INSTRUMENTS GC9790Plus) equipped with thermal conductivity detector (TCD).

4.2 Calculation of products (NH_3, NO_2^- and H_2) Faradaic efficiency (FE) and NH_3 yield

Faradaic efficiency of NH_3 and NO_2^- was calculated using the following equation:

$$FE = \frac{n \times c \times V \times F}{Q} \times 100\%$$

where *n* is the number of electrons transferred (n = 8 for NH_3, n = 2 for NO_2^-), *c* is the concentration of NH_3 or NO_2^- in the catholyte, *V* is the volume of the catholyte (60 mL), *F* is the Faraday constant (96485 C mol^{-1}), and *Q* is the total charge passing the working electrode.

Faradaic efficiency of H_2 was calculated using the standard calculation table of gas chromatograph.

NH_3 yield was calculated using the following equation:

$$Yield(NH_3) = \frac{c \times V}{S \times t}$$

where *c* is the concentration of NH_3 in the catholyte, *V* is the volume of the catholyte (60 mL), *S* is the geometric surface area of the electrode (1 cm^2), and *t* is the electrolysis time (1000 s = 1/3.6 h).

4.3 ^{15}N isotope labeling experiments

To elucidate the origin of ammonia product, $K^{15}NO_3$ (99 atom % ^{15}N) was employed as the nitrogen source. After chronoamperometry test at -0.9 V for 1000 s in 60 mL 1 M KOH solution containing 1.0 g $K^{15}NO_3$ (0.082 M), 500 μL of the reaction electrolyte was collected and mixed with 500 μL of 2 mM maleic acid (dissolved in 1.5 M HCl) and 100 μL of DMSO-d_6. Subsequently, 600 μL of the mixture solution was used for ^1H NMR test on an NMR spectrometer (Bruker AVANCE III 400 MHz). The corresponding standard curve of $^{15}NH_4^+$ was obtained by using a series of standard $^{15}NH_4Cl$ solutions (2, 4, 6, 8 and 10 mM) in the same operation.

4.4 Calculation of electrochemically active surface area (ECSA)

The electrochemical active surface area (ECSA) was determined by analyzing the double-layer capacitance (C_{dl}) from cyclic voltammetry (CV) measurements conducted at scan rates of 10, 20, 30, 40, and 50 mV s^{-1} within a non-Faradaic potential range from 0.6 to 0.7 V. The ECSA of the working electrode was calculated using the following formula:

$$C_{dl} = \frac{\Delta \mathrm{j}}{v}$$

$$ECSA = \frac{C_{dl}}{C_s}$$

where $\Delta j = (j_a - j_c)/2$ at 0.65 V against the scan rates, v is the scan rate, C_{dl} is the double layer capacitance, and C_s is the specific capacitance of the material (C_s is taken as 40 μF cm^{-2} in this study).

4.5 Calculation of H* values

The quantitative comparison of H* values among different catalysts or electrolytes were obtained through cyclic voltammetry (CV) measurements and calculated via the equations below [21]:

$$Q_{\mathrm{H}^*} = S_{\text{integrated area}} \times \frac{\Delta U}{v} \times S_{\text{geometric area}}$$

Wherein, the $S_{\text{integrated area}}$ was obtained from the CV plot, ΔU represents the potential window of the H* desorption peaks, the *v* scan rate was 50 mV s^{-1}, and the geometric area of all the working electrodes was 1 cm^2.

4.6. In situ ATR-FTIR spectra

In situ electrochemical Fourier-transform infrared spectroscopy (ATR-FTIR) measurements were performed on Bruke INVENIO S and an MCT detector. The working electrode was a hemispherical silicon prism coated with a gold layer to enhance the infrared signal, with the Pd-PCOF-3(Cu_3) drop-cast onto its surface. During the experiment, a three-electrode electrochemical cell was used, with a platinum wire as the counter electrode and a Hg/HgO (with 1 M KOH solution) electrode as the reference. The electrolyte was 1 M KOH, continuously saturated with high-purity Ar gas by bubbling during the measurements. The applied potential was scanned at OCP, -0.6 V，-0.7 V，-0.8 V, -0.9 V, -1.0 V, -1.1 V vs RHE.

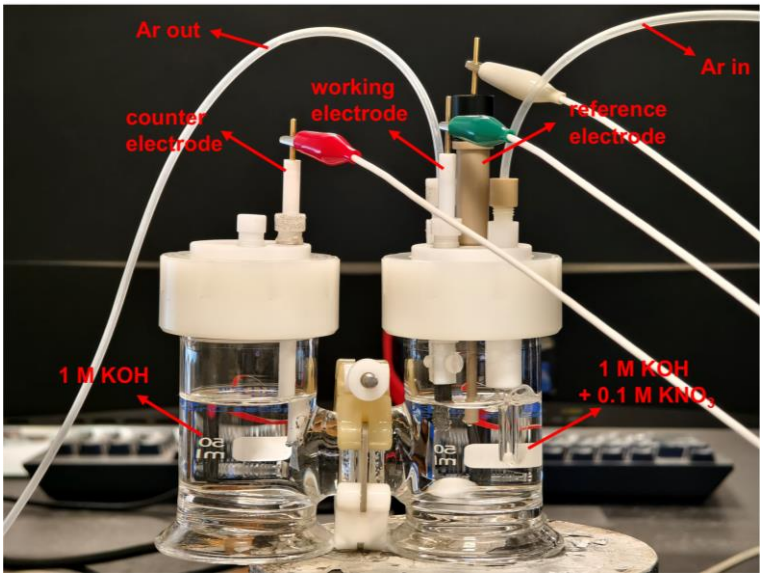

Figure S35. Three-electrode H-type electrolytic cell for NO_3RR.

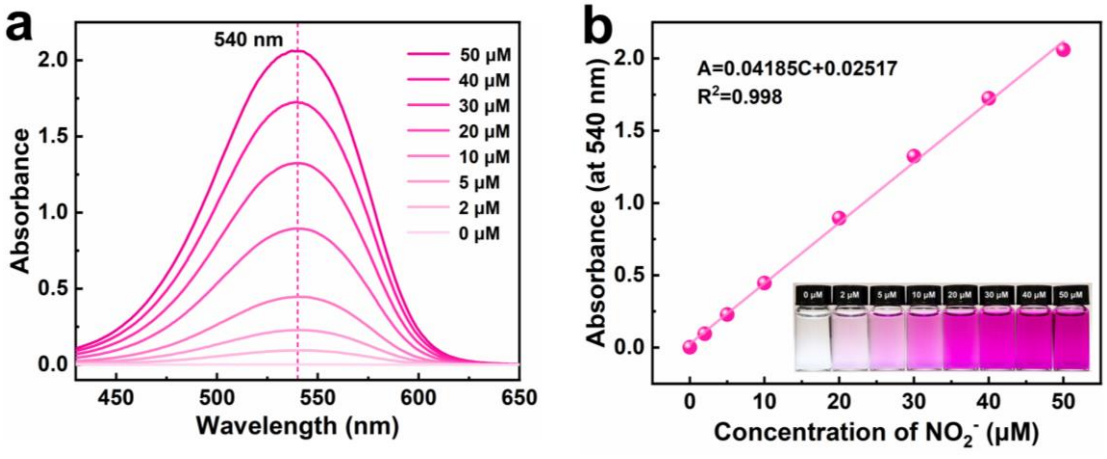

Figure S36. UV-vis absorption spectra of a series of standard KNO_2 solutions (a) and corresponding calibration curve used for the calculation of NO_2^- concentration (b). The inset is the photograph of the KNO_2 solution after chromogenic reaction.

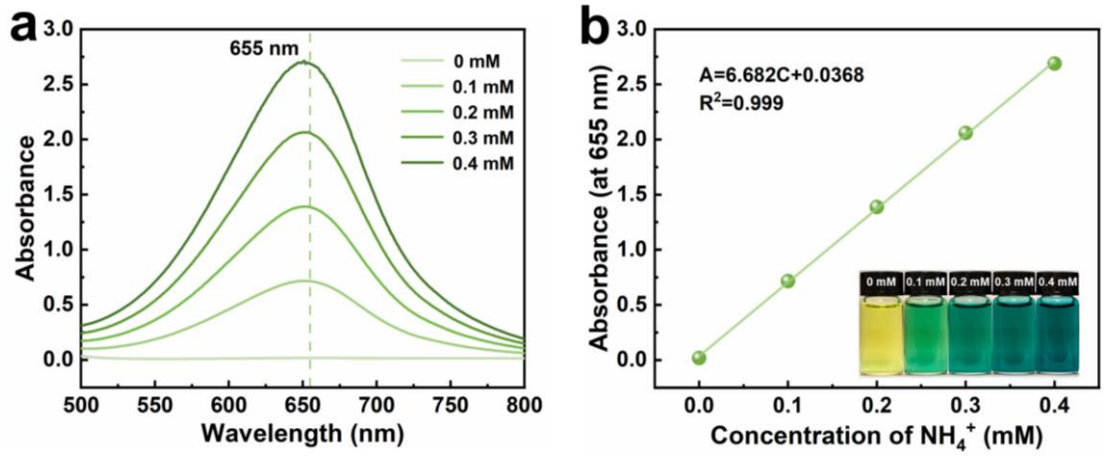

Figure S37. UV-vis absorption spectra of a series of standard NH_4Cl solutions (a) and corresponding calibration curve used for the calculation of NH_3 concentration (b). The inset is the photograph of the NH_4Cl solution after chromogenic reaction.

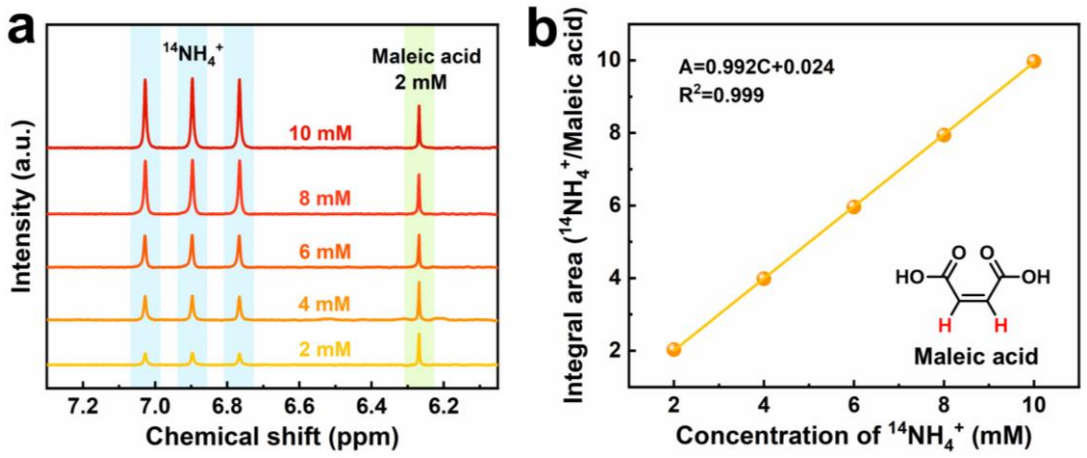

Figure S38. ^{1}H NMR spectra of $^{14}NH_4^+$ ions at different concentrations with 2 mM maleic acid as internal standard (a) and corresponding calibration curve used for the calculation of $^{14}NH_4^+$ concentration (b). The inset is the chemical construction of maleic acid.

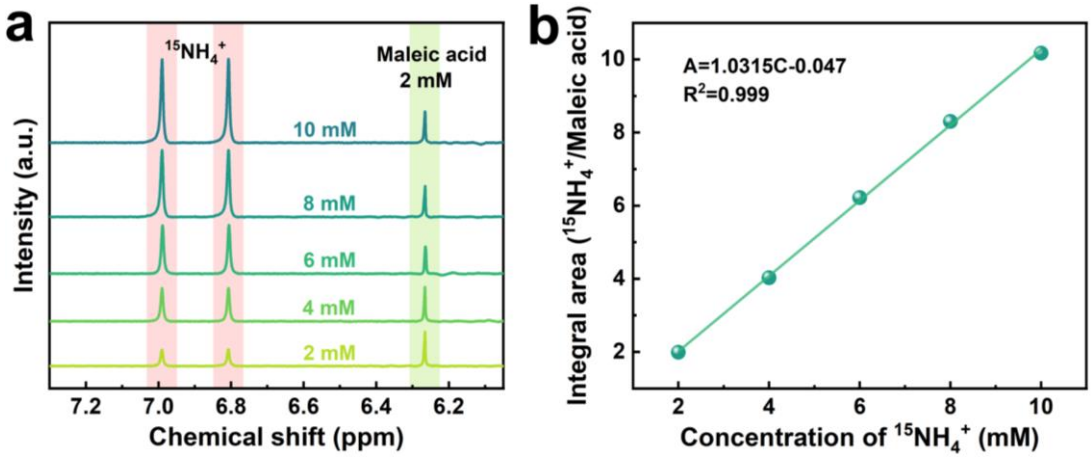

Figure S39. ^{1}H NMR spectra of $^{15}NH_4^+$ ions at different concentrations with 2 mM maleic acid as internal standard (a) and corresponding calibration curve used for the calculation of $^{15}NH_4^+$ concentration (b).

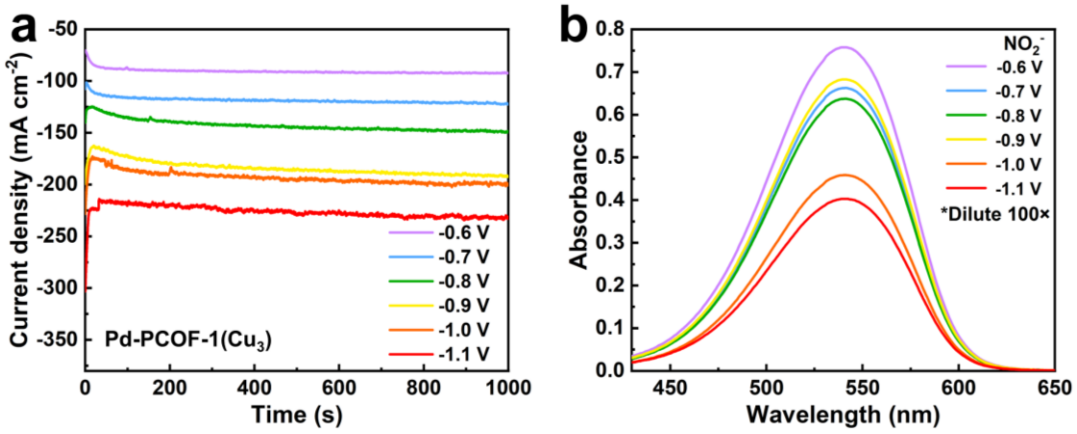

Figure S40. Chronoamperometry curve of Pd-PCOF-1(Cu_3) for NO_3RR at different applied potentials (a). UV-vis absorption spectra of NO_2^- after chromogenic reaction (b).

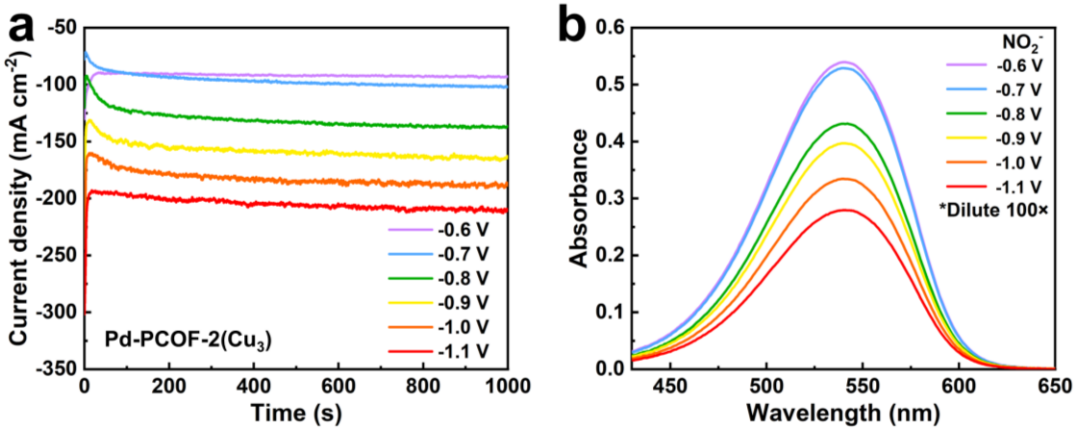

Figure S41. Chronoamperometry curve of Pd-PCOF-2(Cu_3) for NO_3RR at different applied potentials (a). UV-vis absorption spectra of NO_2^- after chromogenic reaction (b).

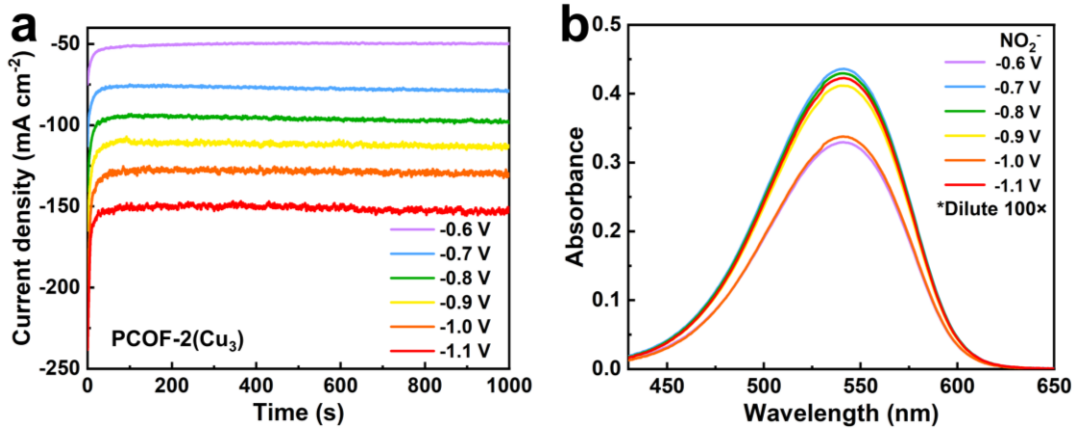

Figure S42. Chronoamperometry curve of PCOF-2(Cu_3) for NO_3RR at different applied potentials (a). UV-vis absorption spectra of NO_2^- after chromogenic reaction (b).

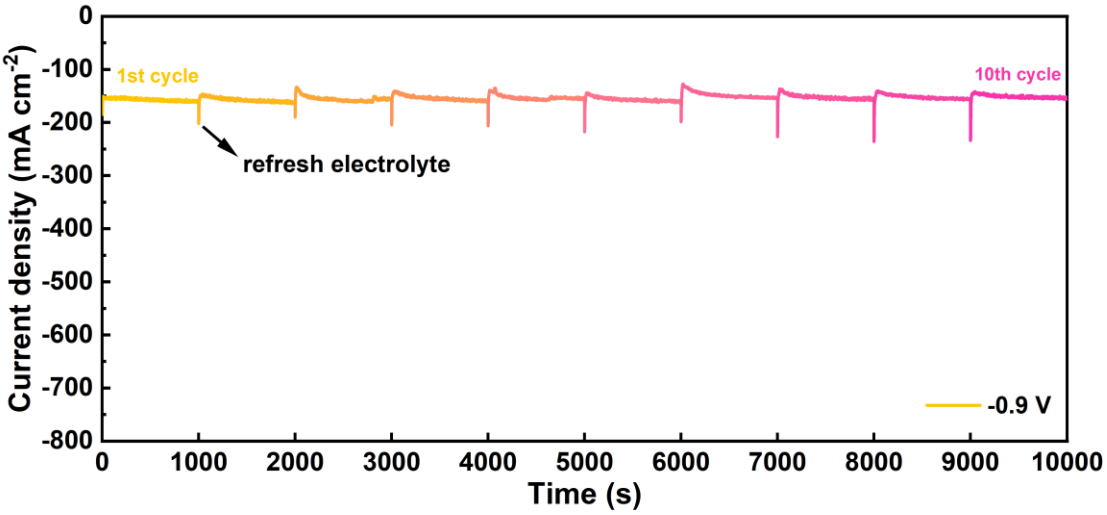

Figure S43. The current density curve of Pd-PCOF-2(Cu_3) for continuous cyclic electrolysis at -0.9 V vs. RHE.

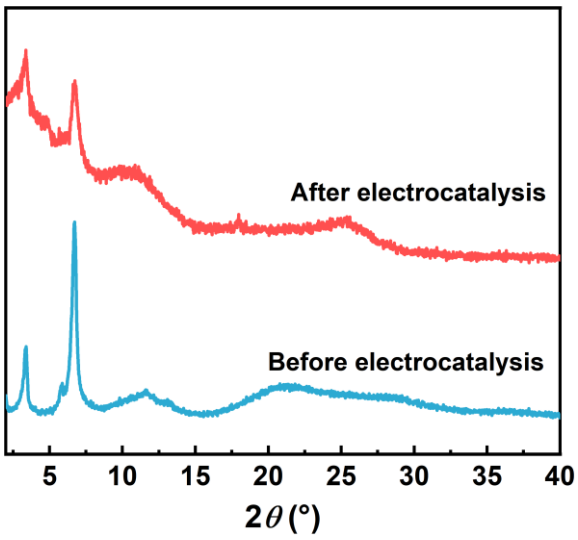

Figure S44. PXRD patterns of Pd-PCOF-2(Cu_3) before and after electrocatalysis 10 consecutive cycles.

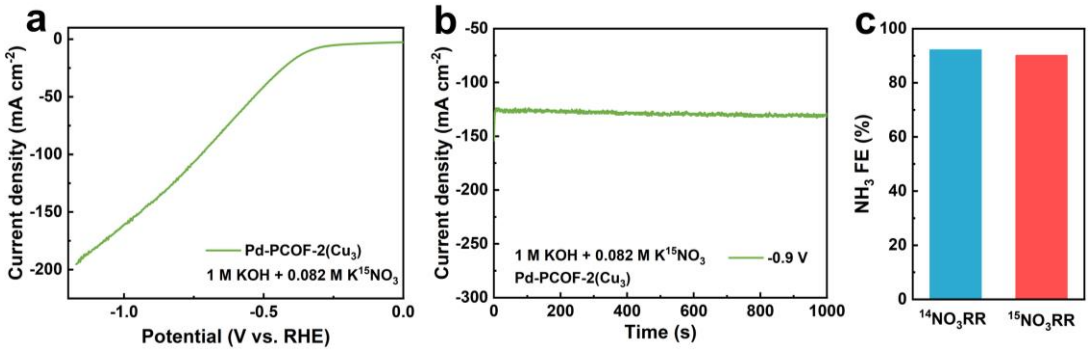

Figure S45. LSV curve at a scan rate of 10 mV s^{-1} (a) and chronoamperometry curve at -0.9 V vs. RHE (b) of Pd-PCOF-2(Cu_3) in 1 M KOH with 0.082 M $K^{15}NO_3$. The NH_3 FE of Pd-PCOF-2(Cu_3) after electrolysis using $^{14}NO_3^-$ or $^{15}NO_3^-$ as nitrogen resources at -0.9 V vs. RHE (c).

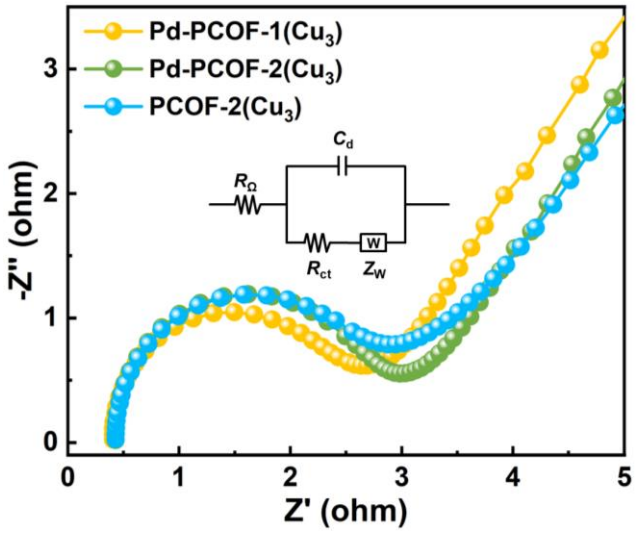

Figure S46. Nyquist plots of Pd-PCOF-1(Cu_3), Pd-PCOF-2(Cu_3) and PCOF-2(Cu_3) in 1 M KOH and containing 0.1 M KNO_3.

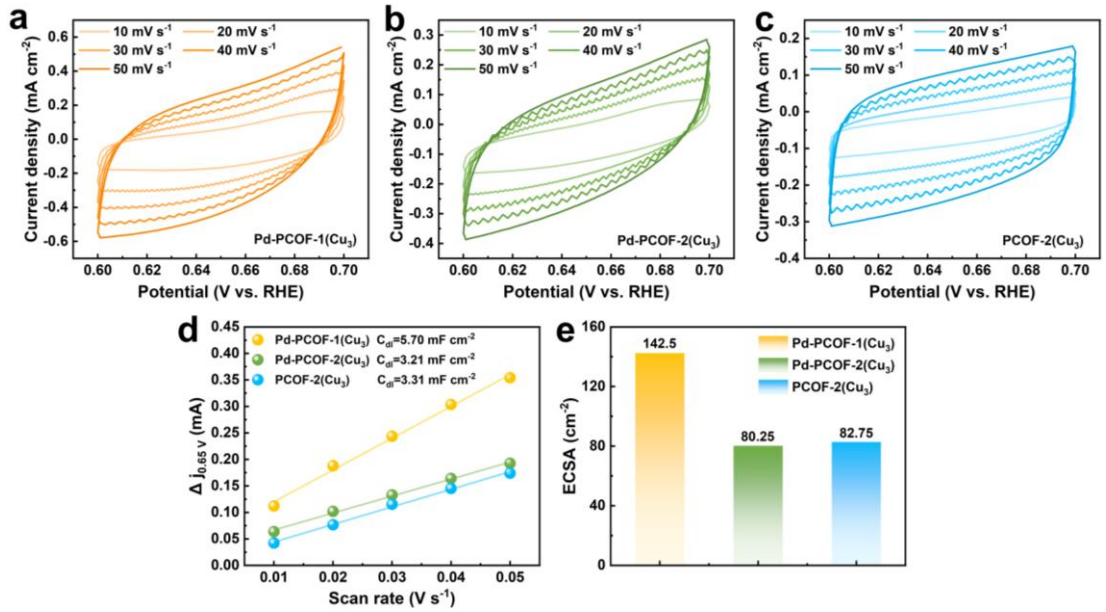

Figure S47. CV curves of Pd-PCOF-1(Cu_3) (a), Pd-PCOF-2(Cu_3) (b) and PCOF-2(Cu_3) (c) at different scan rates. CV current density versus scan rate (the liner slope is equivalent to the C_{dl}) (d). The ECSA comparison of Pd-PCOF-1(Cu_3), Pd-PCOF-2(Cu_3) and PCOF-2(Cu_3) (e).

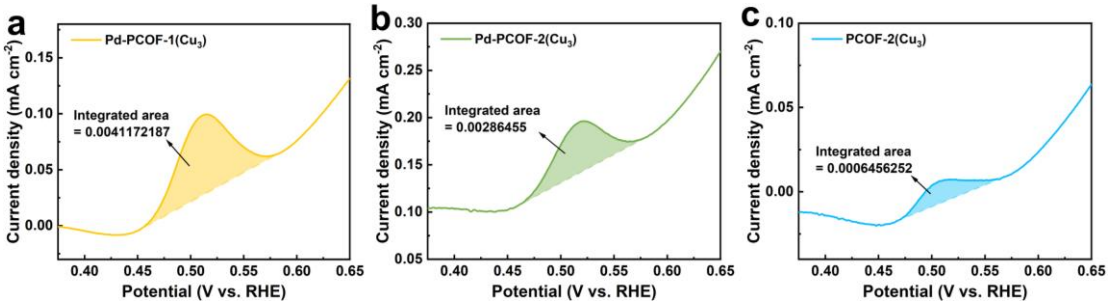

Figure S48. The integrated area of $^{*}H_{ads}$ from the peak of the CV curves over Pd-PCOF-1(Cu_3) (a), Pd-PCOF-2(Cu_3) (b) and PCOF-2(Cu_3) in 1 M KOH.

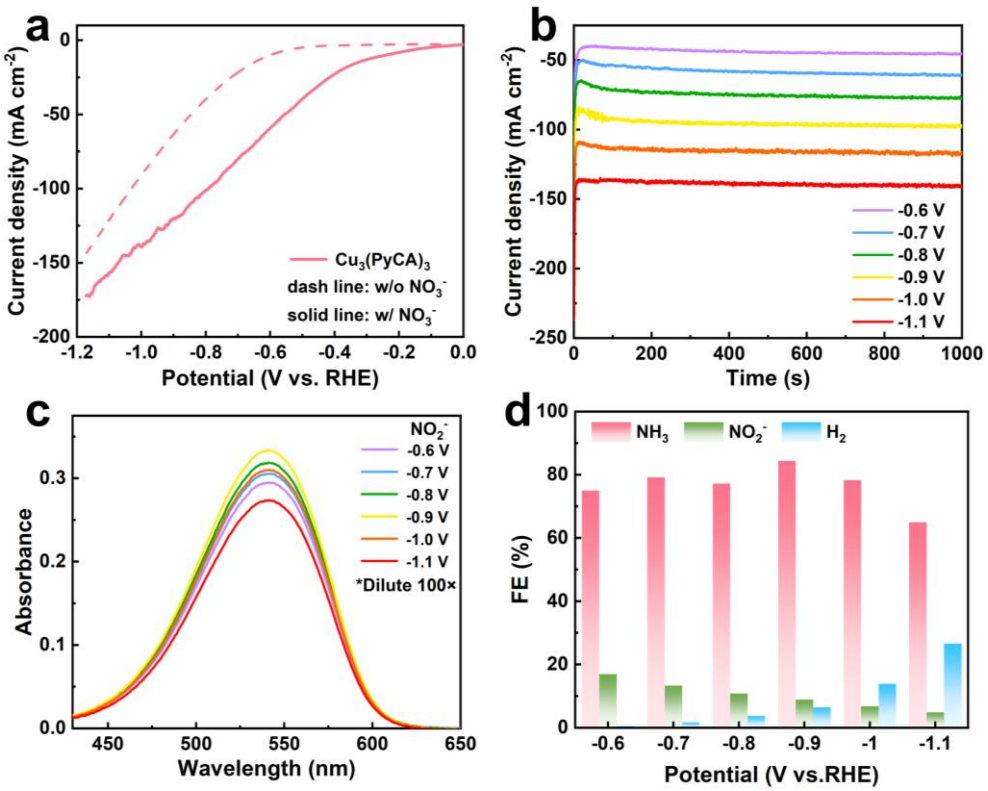

Figure S49. LSV curve at a scan rate of 10 mV s^{-1} (a) and chronoamperometry curve at different applied potentials (b) of $Cu_3(PyCA)_3$ for NO_3RR. UV-vis absorption spectra of NO_2^- after chromogenic reaction (c). NH_3, NO_2^- and H_2 FEs of $Cu_3(PyCA)_3$ at different applied potentials (d).

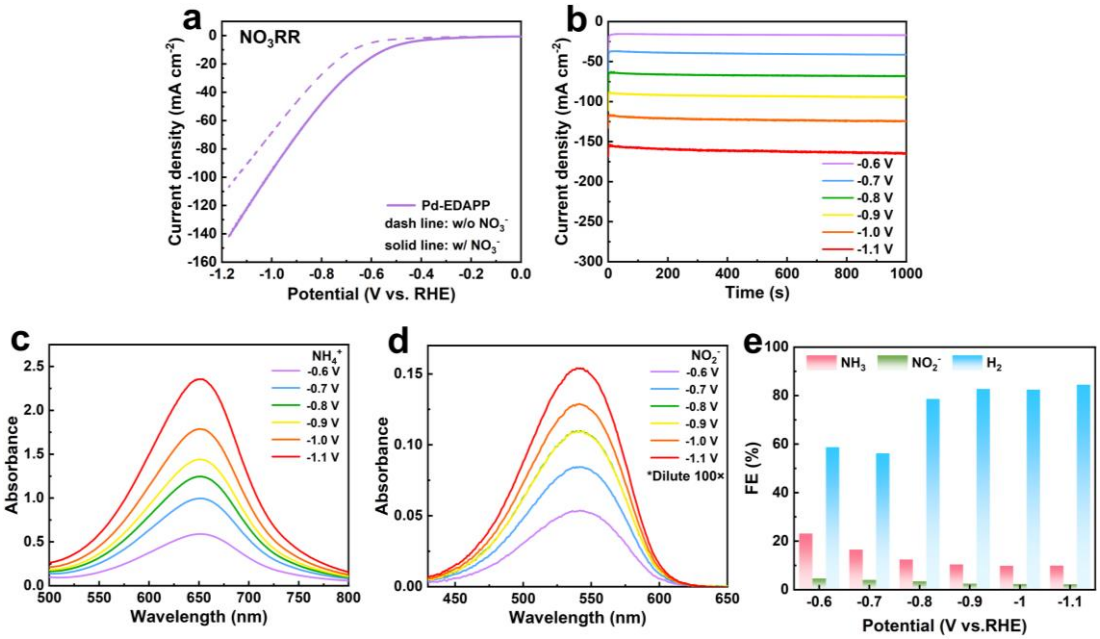

Figure S50. LSV curve at a scan rate of 10 mV s^{-1} (a) and chronoamperometry curve at different applied potentials (b) of Pd-EDAPP for NO_3RR. UV-vis absorption spectra of NH_4^+ (c) and NO_2^- (d) after chromogenic reaction. NH_3, NO_2^- and H_2 FEs of Pd-EDAPP at different applied potentials (e).

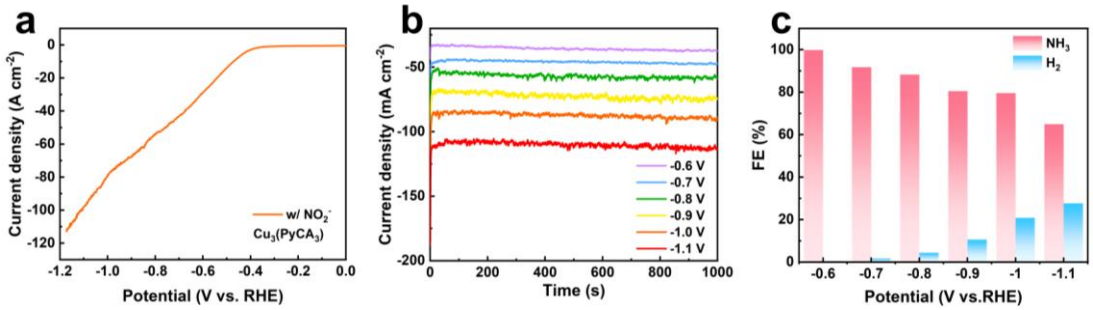

Figure S51. LSV curve at a scan rate of 10 mV s^{-1} (a) and chronoamperometry curve at different applied potentials (b) of $Cu_3(PyCA)_3$ for NO_2RR. NH_3 and H_2 FEs of $Cu_3(PyCA)_3$ at different applied potentials (c).

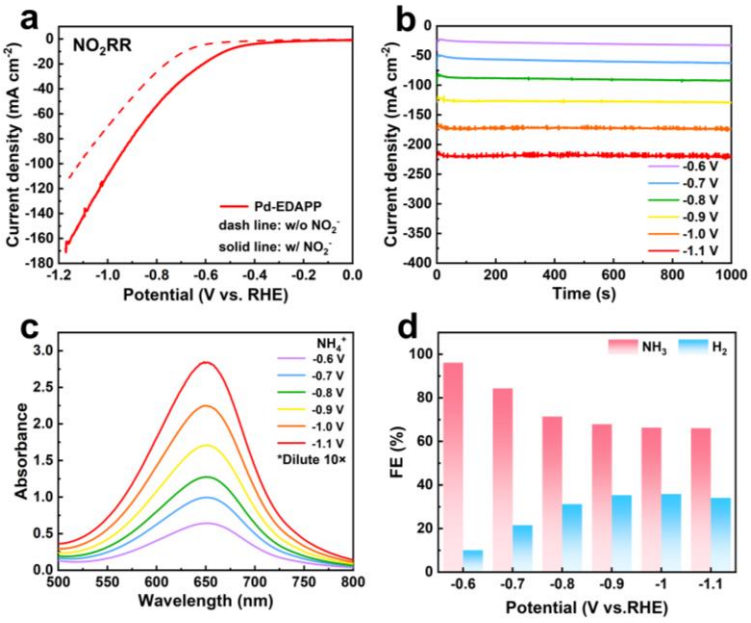

Figure S52. LSV curve at a scan rate of 10 mV s^{-1} (a) and chronoamperometry curve at different applied potentials (b) of Pd-EDAPP for NO_2RR. UV-vis absorption spectra of NH_4^+ (c) after chromogenic reaction. NH_3 and H_2 FEs of Pd-EDAPP at different applied potentials (d).

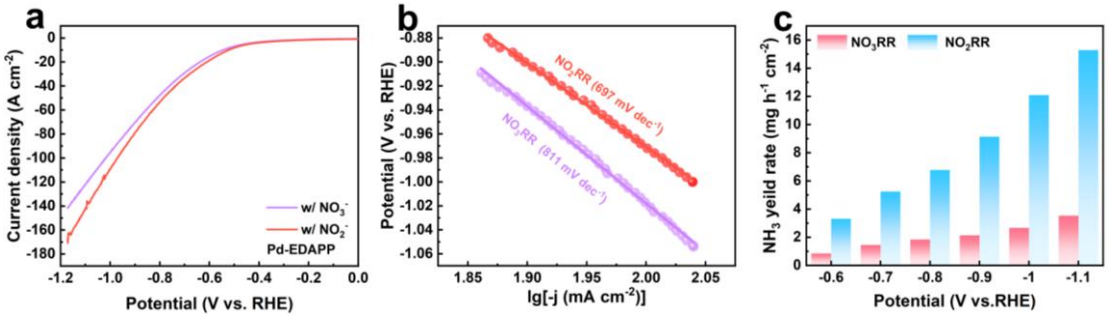

Figure S53. LSV curve at a scan rate of 10 mV s^{-1} of Pd-EDAPP for NO_2RR and NO_3RR (a). The Tafel plots of of Pd-EDAPP for NO_2RR and NO_3RR (b). The generation rate of NH_3 in Pd-EDAPP-catalyzed NO_3RR and NO_2RR at different applied potentials (c).

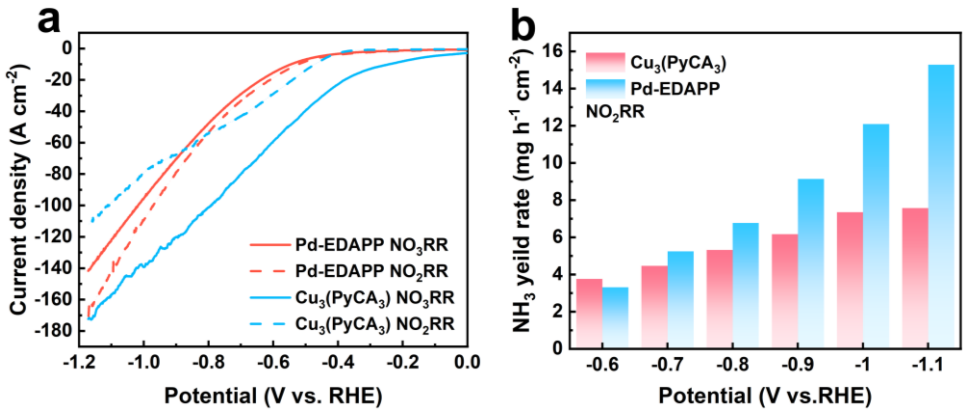

Figure S54. LSV curve at a scan rate of 10 mV s^{-1} of Pd-EDAPP and $Cu_3(PyCA)_3$ for NO_2RR and NO_3RR (a). The NH_3 yield rate of Pd-EDAPP and $Cu_3(PyCA)_3$ for NO_2RR at different applied potentials (b).

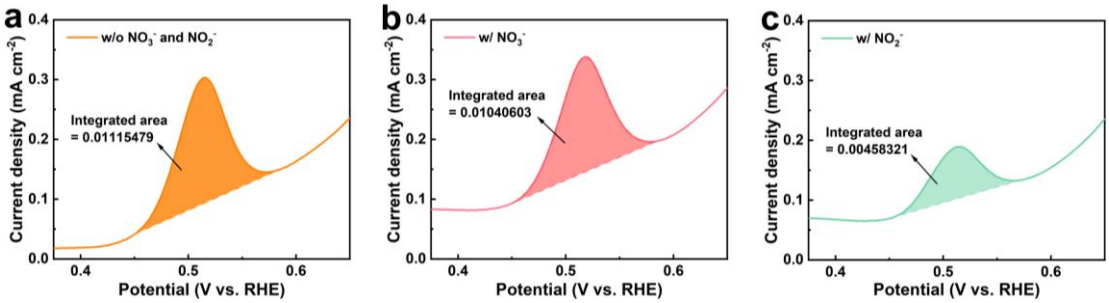

Figure S55. The integrated area of $^*H_{ads}$ from the peak of the CV curves over Pd-EDAPP in 1 M KOH (a) and containing 0.1 M KNO_3 (b) or 0.1 M KNO_2 (c).

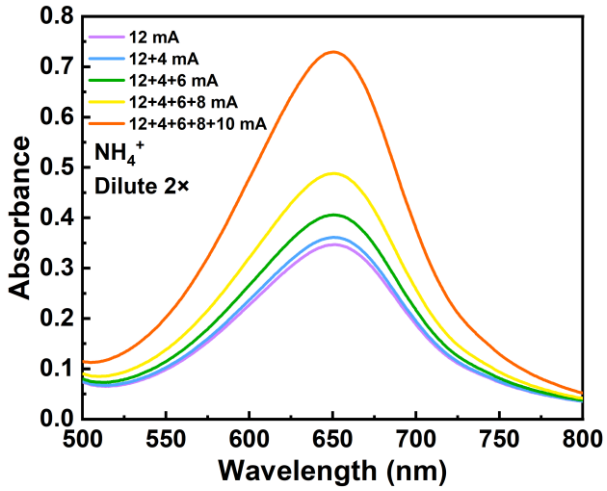

Figure S56. UV-vis absorption spectra of NO_2^- after chromogenic reaction for Zn-NO_3^- battery.

References

[1] F. Lv, M. Sun, Y. Hu, J. Xu, W. Huang, N. Han, B. Huang, Y. Li, *Energy Environ. Sci.*, 2023, **16**, 201-209.

[2] H. Hu, R. Miao, F. Yang, F. Duan, H. Zhu, Y. Hu, M. Du, S. Lu, *Adv. Energy Mater.*, 2024, **14**, 2302608.

[3] J. Zhong, H. Duan, M. Cai, Y. Zhu, Z. Wang, X. Li, Z. Zhang, W. Qu, K. Zhang, D. Han, D. Cheng, Y. Shen, M. Xie, E. Cortes, D. Zhang, *Angew. Chem. Int. Ed.*, 2025, **64**, e202507956.

[4] Y. Zhu, H. Duan, C. Gruder, W. Qu, H. Zhang, Z. Wang, J. Zhong, X. Zhang, L. Han, D. Cheng, A. Medina, E. Cortés, D. Zhang, *Angew. Chem. Int. Ed.*, 2025, **64**, e202421821.

[5] H. Huang, K. Wang, *Green Chem.*, 2023, **25**, 9167-9174.

[6] M. Li, B. Han, L. Gong, Y. Jin, M. Wang, X. Ding, D. Qi, J. Jiang, *Chinese Chemical Letters.*, 2026, **37**, 110590.

[7] S. Mohamed, S. Namvar, T. Zhang, H. Shahbazi, Z. Jiang, A. Rappe, A. Salehi-Khojin, S. Nejati, *Adv. Mater.*, 2024, **36**, 2309302.

[8] X. Li, S. Xia, S. Yang, X. Yang, S. Zheng, X. Xu, Y. Wang, Q. Xu, Z. Jiang, *Angew. Chem. Int. Ed.*, 2025, **64**, e202507479.

[9] Z. Zhang, M. Wang, H. Xing, X. Zhou, L. Gao, S. Chen,Y. Chen, H. Xu, W. Li, S. Yuan, C. Li, Z. Jin, J. Zuo, *Angew. Chem. Int. Ed.*, 2025, **64**, e202505580.

[10] Z. Zhang, Y. Lv, Y. Gu, X. Zhou, B. Tian, A. Zhang, Z. Yang, S. Chen, J. Ma, M. Ding, J. Zuo, *Angew. Chem. Int. Ed.*, 2025, **64**, e202418272.

[11] L. Xie, Q. Hao, Y. Wu, H. Qin, L. Zheng, K. Liu, *Appl Catal B Environ.*, 2020, **375**, 125428.

[12] Y. Zou, Y. Yan, Q. Xue, C. Zhang, T. Bao, X. Zhang, L. Yuan, S. Qiao, L. Song, J. Zou, C. Yu, C. Liu, *Angew. Chem. Int. Ed.*, 2024, **63**, e202409799.

[13] S. Tian, R. Wu, H. Liu, C. Yan, Z. Qi, P. Song, W. Chen, L. Song, Z. Wang, C. Lv, *Angew. Chem. Int. Ed.*, 2025, **64**, e202510665.

[14] M. Wang, S. Li, Y. Gu, W. Xu, H. Wang, J. Sun, S. Chen, Z. Tie, J. Zuo, J. Ma, J. Su, Z. Jin, *J.Am.Chem. Soc.*, 2024, **146**, 20439-20448.

[15] M. Wang, Y. Meng, W. Xu, T. Shen, Y. Wang, Q. Yu, C. Liu, Y. Gu, Z. Tie, Z. Fan, J. Zuo, J. Su, Z. Jin, *J. Am. Chem. Soc.*, 2025, **147**, 18327-18337.

[16] P. Muthukumar, Z. Ullah, X. Zhang, H. Ullah, Y. Liu, L. Li, S. Tian, X. Zhou, S. Anthony, Y. Zuo, C. Lv, X. Wang, C. Wang, *J. Am. Chem. Soc.*, 2025, **147**, 29949-29960.

[17] P. Liu, J. Yan, H. Huang, W. Song, *Chemical Engineering Journal.*, 2023. **466**, 143134.

[18] X. Fu, H. Guo, D. Si, H. Zhu, Y. Lan, Y. Huang, R. Cao, *Chem. Sci.*, 2025, **16,** 13503.

[19] H. Lin, Q. Mo, Y. Wang, C. Chen, L. Zhang, *Inorg. Chem*., 2025, **64**, 6, 2669–2680.

[20] X. Li, J. Wang, F. Xue, Y. Wu, H. Xu, T. Yi, Q. Li, *Angew. Chem. Int. Ed.*, 2021, **60**, 2534-2540.

[21] H. Wang, M. He, R. Li, Y. Liu,Y. Gao, B. Zhang, C. Liu, *Angew. Chem. Int. Ed.*, 2025, e202513463.